Journal of the Association for Research in Otolaryngology

Polarity sensitivity as a potential correlate of neural degeneration in cochlear implant users.

--Manuscript Draft--

Manuscript Number:	JARO-D-19-00038R2
Full Title:	Polarity sensitivity as a potential correlate of neural degeneration in cochlear implant users.
Article Type:	Original Article
Keywords:	cochlear implant; polarity; neural health; computed tomography scans
Corresponding Author:	Quentin Mesnildrey, Ph.D Aix-Marseille Univ, Centrale Marseille, CNRS, LMA, Marseille Marseille cedex 13, FRANCE
Corresponding Author Secondary Information:	
Corresponding Author's Institution:	Aix-Marseille Univ, Centrale Marseille, CNRS, LMA, Marseille
Corresponding Author's Secondary Institution:	
First Author:	Quentin Mesnildrey, Ph.D
First Author Secondary Information:	
Order of Authors:	Quentin Mesnildrey, Ph.D
	Frédéric Venail
	Robert P Carlyon
	Olivier Macherey
Order of Authors Secondary Information:	
Funding Information:	
Abstract:	Cochlear implant (CI) performance varies dramatically between subjects. Although the causes of this variability remain unclear, the electrode-neuron interface is thought to play an important role. Here we evaluate the contribution of two parameters of this interface on the perception of CI listeners: the electrode-to-modiolar wall distance (EMD), estimated from cone-beam computed tomography (CT) scans, and a measure of neural health. Since there is no objective way to quantify neural health in CI users we measure stimulus polarity sensitivity, which is assumed to be related to neural degeneration, and investigate whether it also correlates with subjects' performance in speech recognition and spectro-temporal modulation detection tasks. Detection thresholds were measured in fifteen CI users (sixteen ears) for partial-tripolar triphasic pulses having an anodic or a cathodic central phase. The polarity effect was defined as the difference in threshold between cathodic and anodic stimuli. Our results show that both the EMD and the polarity effect correlate with detection thresholds, both across and within subjects, although the within-subject correlations were weak. Furthermore, the mean polarity effect, averaged across all electrodes for each subject was negatively correlated with performance on a spectro-temporal modulation detection task. In other words, lower cathodic thresholds were associated with better spectro-temporal modulation detection performance, which is also consistent with polarity sensitivity being a marker of neural degeneration. Implications for the design of future subject-specific fitting strategies are discussed.

Title:

Polarity sensitivity as a potential correlate of neural degeneration in cochlear implant users[1].

Authors:

- Quentin Mesnildrey[a] (corresponding author, ORCID: 0000-0003-2149-3599);
- Frédéric Venail[b];
- Robert P. Carlyon[c];
- Olivier Macherey[a].

Affiliations:

a- Aix-Marseille Univ., Centrale Marseille, CNRS, LMA, Marseille, France.
b- ENT Department and University Hospital, Montpellier, France.
c- Medical Research Council, Cognition and Brain Sciences Unit, University of Cambridge, United Kingdom.

Key words:

cochlear implant, polarity, neural health, computed tomography scans

Abstract

Cochlear implant (CI) performance varies dramatically between subjects. Although the causes of this variability remain unclear, the electrode-neuron interface is thought to play an important role. Here we evaluate the contribution of two parameters of this interface on the perception of CI listeners: the electrode-to-modiolar wall distance (EMD), estimated from cone-beam computed tomography (CT) scans, and a measure of neural health. Since there is no objective way to quantify neural health in CI users we measure stimulus polarity sensitivity, which

[1] Part of this work was presented at the Conference on Implantable Auditory Prostheses in Lake Tahoe, California, 2017

is assumed to be related to neural degeneration, and investigate whether it also correlates with subjects' performance in speech recognition and spectro-temporal modulation detection tasks. Detection thresholds were measured in fifteen CI users (sixteen ears) for partial-tripolar triphasic pulses having an anodic or a cathodic central phase. The polarity effect was defined as the difference in threshold between cathodic and anodic stimuli. Our results show that both the EMD and the polarity effect correlate with detection thresholds, both across and within subjects, although the within-subject correlations were weak. Furthermore, the mean polarity effect, averaged across all electrodes for each subject was negatively correlated with performance on a spectro-temporal modulation detection task. In other words, lower cathodic thresholds were associated with better spectro-temporal modulation detection performance, which is also consistent with polarity sensitivity being a marker of neural degeneration. Implications for the design of future subject-specific fitting strategies are discussed.

Number of tables: 2

Number of figures: 10

1 Introduction

Several studies have shown that the variability in performance of cochlear implant (CI) users is at least partly due to differences in the electrode-neuron interface (Bierer and Faulkner, (2010); Cosentino et al., (2016); Garadat et al., (2010)). A conceptual model of this interface involves (1) the electrode position, (2) the current path from the electrode to the neurons and (3) the distribution of the neural population. While (1) and (2) can respectively be investigated by analyzing CT images (Saunders et al., (2002); Cohen et al., (2006); Long et al., (2014); van der Marel et al., (2015); Venail et al., (2015)) and by performing electrical measurements (Spelman et al., (1982); Vanpoucke et al., (2004); Micco and Richter, (2006); Mesnildrey et al., (2019)) assessing neural health remains a challenge.

Studies counting the remaining cells in cadaver cochleas showed the complexity of predicting neural health in CI patients, because the speed of neural degeneration depends on numerous factors such as the duration and etiology of deafness (Nadol et al., (1989); Linthicum and

Anderson, (1991); Glueckert et al., (2005)). In addition, and rather surprisingly, studies that examined the correlation between the number of remaining nerve fibers and speech performance have yielded inconsistent results (Khan et al., (2005); Fayad and Linthicum, (2006); Nadol and Eddington, (2006); Kamakura and Nadol, (2016)).

Since it is currently not possible to objectively quantify neural survival in CI users, several studies have tried to identify psychophysical or electrophysiological correlates. Pfingst et al., (2004) and Long et al., (2014) reported correlations between the within-subject variance in threshold across the electrode array and speech performance. They argued that a large threshold variance across the array may reflect the presence of neural dead regions, which would negatively impact speech perception. Zhou and Pfingst, (2014) measured the effect of electrical pulse rate on threshold, termed multipulse integration, in human CI users. They proposed, based on similar experiments in animals (Pfingst et al., (2011)), that the decrease in threshold associated with a doubling of the pulse rate could be a psychophysical correlate of neural health. Consistent with this hypothesis, they reported that the amplitude of the multipulse integration was positively correlated with consonant recognition in noise.

Animal studies by Prado-Guitierrez et al., 2007 and Ramekers et al., 2014 examined the effect of two parameters - the inter-phase gap and the phase duration - on the amplitude of the electrically-evoked compound action potential (eCAP). Prado-Guitierrez et al., (2007) reported that the increase in eCAP amplitude as a function of both the inter-phase gap and the phase duration was larger in healthy cochleas. The same relationship was found in Ramekers et al., (2014) for the inter-phase gap only.

A modelling study by Rattay, (1999) investigated the response of single nerve fibers to electrical stimulation. They predicted that the site of excitation along the nerve fibers should depend on stimulus polarity. In particular, they showed that cathodic stimulation tends to yield longer latencies than anodic stimulation for it is more likely to initiate action potentials at the peripheral processes. Similar observations were made by Rattay et al., (2001) and more recently by Resnick et al., (2018). Another important result from Resnick et al., (2018) is that a partial demyelination of peripheral processes reduces its excitability and yields an incease in threshold for cathodic but not for anodic stimulation. Polarity sensitivity may thus directly relate to the state of degeneration or demyelination of the peripheral processes. Since neural degeneration is retrograde by nature (Spoendlin, (1975)), it is also possible that the regions with a lot of peripheral degeneration are also regions where the number of surviving neurons is low. As a result, one may assume polarity sensitivity to relate to the local state of the neural population. More specifically, a relatively higher sensitivity to anodic stimulation compared to cathodic stimulation may reflect a site with high neural degeneration.

Polarity sensitivity can be assessed in human CI users by means of asymmetric pulse shapes, such as pseudomonophasic or triphasic pulses (Figure 1, Bonnet et al., (2004); Eddington et al., (2004); Macherey et al., (2008), (2006)). Unlike clinical symmetric biphasic pulses, such asymmetric pulse shapes can induce a domination of one polarity over the other, while maintaining electrical charge balance (Carlyon et al., (2013)). Macherey et al., (2017) demonstrated that polarity sensitivity at detection threshold can differ across human CI users, or across electrodes for a given subject. These differences have also been assumed to relate to the state of neural degeneration or demyelination of the peripheral processes.

Based on these studies, measuring polarity sensitivity across the electrode array has recently been proposed as an estimate of neural health along the cochlea (Carlyon et al., (2018); Hughes et al., (2018)).

Here we measure the polarity effect, defined as the difference in threshold between cathodic (Fig. 1.B) and anodic (Fig. 1.C) stimulation. Our first aim is to investigate how it relates to overall sensitivity across the electrode array (detection threshold). Furthermore, computational modeling by Rattay et al., (2001) predicts that the polarity effect may also depend on the position of the electrode in the scala tympani. Given that detection thresholds have also been shown to depend on the electrode-to-modiolar wall distance (EMD), we estimate this distance in a subset of our subjects from whom scans are available. This allows us to study the separate contributions of the EMD and of the polarity effect on overall sensitivity. Finally, assuming the polarity effect is a correlate of neural health, we would expect it to be related to overall performance on suprathreshold tasks. A second aim of the present study is to correlate the polarity effect with performance on speech perception tasks and/or to measures of spectro-temporal modulation discrimination (Won et al., (2007); Aronoff and Landsberger, (2013)). We hypothesize that a large positive polarity effect reveals poor neural health while a negative polarity effect reveals good neural health. We would thus expect the performance on suprathreshold tasks to be negatively correlated with the polarity effect.

Another measure of interest concerns the variation in threshold across electrodes. Long et al., (2014) measured detection thresholds, EMD and speech recognition in a group of CI users implanted with an experimental version of the device manufactured by Cochlear Corporation. For seven of their ten subjects, detection thresholds were positively correlated with the EMDs, referred to as the distance model. Interestingly, speech recognition scores were correlated with the residuals of the distance model, meaning that when the distance could not explain the variation in threshold across electrodes, speech performance tended to be poorer. They hypothesized that this might reflect the irregularity of neural health across the electrode array. Here we also aim to replicate this experiment with a different CI group implanted with a device from a different manufacturer.

2 Methods

2.1 Subjects

Experiments were conducted both in Marseille (France) and in Cambridge (United Kingdom) with a total of 15 adult CI users (16 ears) whose details are reported in Table 1. Ten subjects (11 ears) were tested in Marseille and five were tested in Cambridge. All subjects were implanted with a CII/HiRes 90k device manufactured by Advanced Bionics. Their electrode array was the HiFocus 1j except for subjects S2(L) and AB9 who had the MidScala electrode. The labels S2(L) and S2(R) refer to the left and right ears of the same bilaterally-implanted subject. In the following, the data corresponding to each ear were treated as separate data sets. Subjects were paid for their participation. All experiments were approved by the ethics committees (Marseille: Eudract 2012-A00438-35; Cambridge: 00/327).

2.2 Detection thresholds

Detection thresholds were measured for all subjects using the Bionic Ear Data Collection System (BEDCS, Advanced Bionics, Litvak, (2003)) and custom Matlab interfaces.

Stimuli

Electrical stimuli were 300-ms pulse trains presented at a rate of 100 pulses per second. Three pulse shapes were used (Figure 1): Cathodic-first symmetric biphasic pulses (CA), triphasic pulses with a cathodic central phase (ACA) and triphasic with an anodic central phase (CAC). The triphasic pulse shapes consisted of a central phase of a given polarity and amplitude, preceded and followed by opposite-polarity phases of the same duration and half the amplitude so as to maintain charge-balancing. ACA and CAC pulses were intended to enhance the influence of the cathodic and anodic phase respectively (Eddington et al., (2004); Carlyon et al., (2013); Macherey and Cazals, (2016)). Henceforth, ACA and CAC thresholds are referred to as cathodic and anodic thresholds, respectively. For all pulse shapes, the duration of each phase was 97 µs.

Stimuli were presented in partial tripolar (pTP) configuration with 75% of the current returning to the flanking electrodes and 25% to the ground (i.e. σ = 0.75, Jolly et al., (1996); Litvak et al., (2007)). Forward-masking experiments have provided evidence that pTP may produce a more spatially-focused stimulation than MP (Bierer et al., (2011); Landsberger et al., (2012)). We thus expected detection thresholds to reflect the responsiveness of restricted portions of the auditory nerve.

In pTP stimulation mode, the most apical and most basal electrodes cannot be stimulated because they do not have two neighboring electrodes, thereby limiting the maximum number of available tripolar channels to 14 (central electrodes ranging from E2 to E15). Any electrode deactivated in the patients' clinical maps (see table 1) was not tested (neither as central electrodes nor as flanking electrodes).

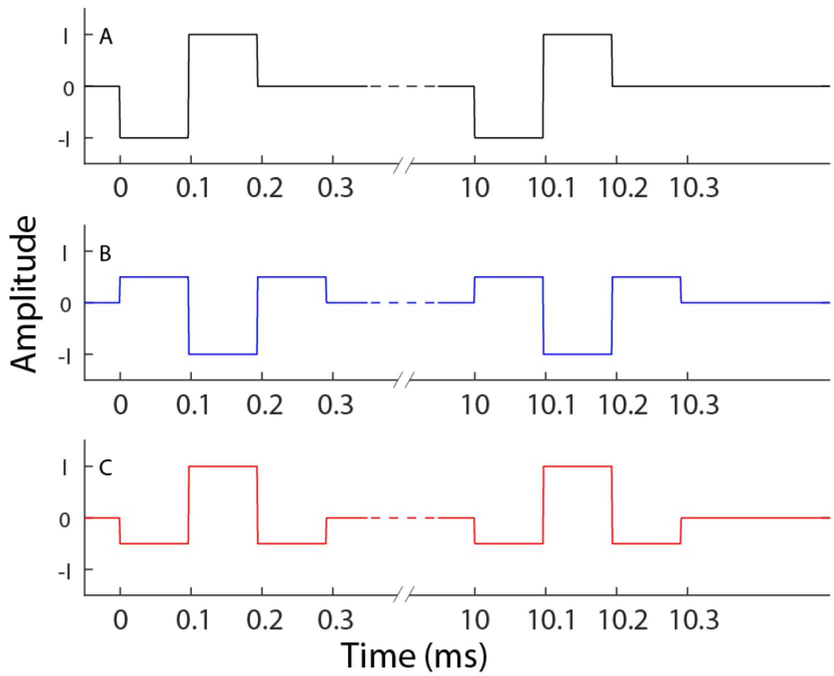

Figure 1: Electrical pulse shapes used for threshold measurements. Panel A: cathodic-first biphasic pulses (CA). Panel B: triphasic cathodic pulses (ACA). Panel C: triphasic anodic pulses (CAC).

Procedure

For most subjects the number of conditions was 42 ({14 electrodes}×{3 pulse shapes}) but this was reduced when an electrode was deactivated in the subject's clinical map (Table 1). Subject AB5, for whom an electrode in the middle of the array was deactivated, was tested on 11 electrodes (total of 33 conditions). The duration of a session only enabled one measure per condition. The thresholds for even and odd electrodes were measured separately yielding two blocks of 7 electrodes and 21 testing conditions. This procedure was chosen, first, to introduce a break approximately half-way through the session and, second, to be able to run independent analysis for both sets of electrodes, which will provide a control on the reliability of the measures. For each subset, one electrode was randomly selected and the three pulse shapes were tested successively, also in a randomized order. The most comfortable level (MCL) was then estimated for each specific condition.

Subjects were asked to report the perceived loudness using a loudness chart ranging from 0 to 10, where 1 corresponds to the quietest just noticeable sound, 6 to the MCL and 10 to sounds that are too loud. The stimulation level was manually increased with an amplitude step of 1 dB starting at a subthreshold level. Typically, when the loudness reached level 2, the amplitude step was reduced to 0.5 dB up to loudness level 4 and then further reduced to 0.2 dB until the MCL was reached. Before each stimulation, it was checked that the current level did not exceed the compliance limit (7 Volts) of the device. If the compliance limit was reached before the MCL, the procedure was stopped and the maximum current level allowed was recorded.

After measuring the MCLs for all 21 conditions, detection thresholds were obtained for each condition using a one-up/one-down procedure. A single 300-ms stimulus was played at an initial level corresponding to 90% of the MCL (or 90% of the maximum level below the compliance limit). Subjects were asked to press the space bar of a computer keyboard when they heard a sound. If a percept was reported within a three-second time window, a lower-amplitude stimulus was played after a random delay ranging between two and three seconds. In the absence of a response after three seconds, a higher-amplitude stimulus was played after a shorter random delay (between 0.1 s and 0.6 s). As a result, with or without a response, the duration between two consecutive stimuli varied between two and six seconds. This timing was chosen after a pilot experiment because it appeared to be a good compromise for a relatively fast procedure while giving the subjects enough time to respond.

Note that, although thresholds obtained with this procedure may have been affected by differences in response criterion between subjects, this would not be expected to influence the difference between anodic and cathodic thresholds.

During this automatic procedure, the incremental/decremental step in level was ± 0.5 dB until the first reversal and ± 0.2 dB afterwards. The procedure stopped after eight reversals and each threshold was calculated as the average of the last six reversals.

2.3 Speech recognition

Depending on the testing location, speech recognition was measured in a sound-insulated booth or in an anechoic chamber using the subjects' own speech processor and clinical map. Two lists of single words (i.e. 100 words in total) from the French (N=9) or British (N=5) versions of the Phonetically Balanced Kindergarten corpus (PBK, Haskins, 1949) were presented to each individual listener. S2 is an American English speaker and thus did not participate in this task. Acoustic stimuli were played in free field through a Fostex 6301B loudspeaker without masking noise. Subjects sat one meter away from the loudspeaker, where the sound pressure level was adjusted to 65 dB. They were asked to repeat each word they heard. Correct and incorrect responses were scored by an experimenter sitting next to the subject and no feedback was provided.

2.4 Spectro-temporally Modulated Ripple Test, (SMRT)

In this study, apart from different native languages, CI users also had a wide variability of experience with their device (see table 1). CI experience varied from 0.5 to 15 years and some of the subjects were prelingually deaf (S5 and S10). To limit the effect of CI experience (Blamey et al., (2013)) and of native language, a spectro-temporally modulated ripple test (SMRT, Aronoff and Landsberger, (2013)) which reflects the ability of subjects to receive and integrate spectro-temporal cues, was also carried out with all 15 subjects. This test and similar ones have been shown to correlate with speech recognition performance in CI users (Won et al., (2007); Lawler et al., (2017)).

The SMRT test is implemented as a 3-interval, 3 alternative forced choice adaptive procedure. Two of the intervals contain a reference stimulus and one contains the target stimulus. The reference has a constant density of 20 ripples per octave (rpo) while the target has an initial density of 0.5 rpo. A one-up/one-down adaptive procedure runs with steps of 0.2 rpo until the subject cannot differentiate the target from the reference. Thresholds are given based on the average of the last six reversals and are expressed in number of rpo. For this test, subjects also used their own processor and clinical map. Stimuli were presented in the same experimental conditions as in the speech recognition experiment (i.e. free field acoustic stimulation at a level of 65 dB SPL). After one run of training with feedback, two additional test runs were carried out without feedback and the outcome measure is given as the average of these two test runs.

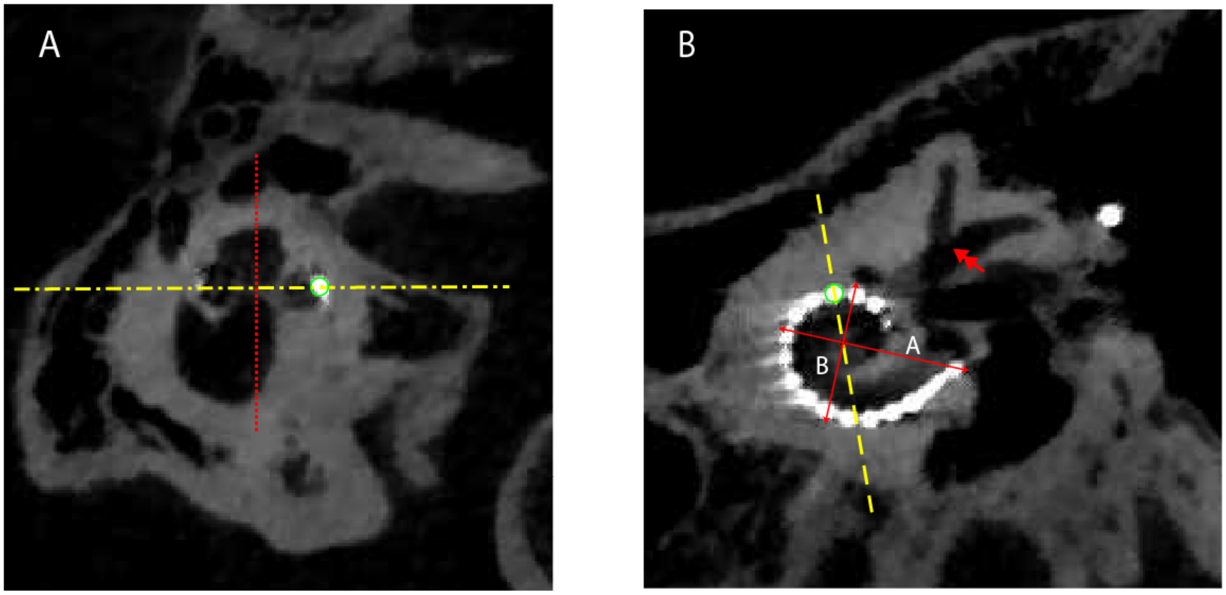

Figure 2: Panel A: vertical section view of the implanted cochlea. The red dotted line represents the modiolar axis, the yellow dash-dotted line represents the horizontal section plane corresponding to panel B. Panel B: Horizontal section of the basal turn of the cochlea. Dashed line: vertical section plane corresponding to panel A. Double arrow head: superior and lateral semicircular canals. The green circle in both panels mark the same electrode

2.5 Electrode-to-modiolar wall distance

The CT scans (Cone beam 5G Newtom, $125\mu\mathrm{m} \times 125\mu\mathrm{m} \times 125\mu\mathrm{m}$ voxels) from 10 ears (S1-2(R)-2(L)-4-5-7-8-10-11-17), were analyzed using the Onis Pro software (v2.5 DigitalCore®, Co. LTD) in order to estimate the electrode-to-modiolar wall distance, (EMD).

CT images were oriented using the method described in Escudé et al., (2006). The 3D manipulating tool was used in order to visualize the basal turn of the cochlea, the vestibule and the anterior branches of the lateral and superior semicircular canals. We marked the largest distance from the round window through the modiolus to the lateral wall (distance A on Fig. 2), and the largest distance perpendicular to A (distance B on Fig. 2). The modiolar axis was defined as the intersection of A and B. In the following, the view perpendicular to the modiolar axis (Fig. 2B) is referred to as the horizontal view and the mid-modiolar sections are referred to as vertical views (Fig. 2A).

As in Escudé et al., (2006) and Pelliccia et al., (2014), the image orientation was validated using both the horizontal and vertical views. Note that the image orientation was made by considering the cochlear geometry rather than the electrode array. The image contrast was then adjusted to offer the best representation of both the modiolar wall and the electrode. Here again the position of the modiolar wall located using one view was validated using orthogonal views.

The position of each electrode was assumed to be at the center of the artifact. Prior to the EMD measurements, the CT images were rotated around the modiolar axis in order to visualize the specific electrode on both horizontal and vertical section views. The green circles in Fig. 2 identify the same electrode in both the horizontal and vertical views.

The EMD was then measured using the software measuring tool as the radial distance from the electrode to the modiolar wall (as revealed by a higher contrast). Again EMD estimations were validated using both horizontal and vertical views. Two independent sets of EMD estimations were made by two observers. Since, in humans, spiral ganglion cells (SGCs) are clustered in Rosenthal's canal, this measurement gives a first approximation of the distance between the electrodes and the SGCs.

2.6 Testing Session

Threshold measurements, speech recognition test and SMRT were carried out in the same session lasting approximately three hours. The subjects were divided in two groups (A and B). Group A started with measurements on the even electrodes while group B started with measurements on the odd electrodes. Each session was organized as follows:

1. MCL estimation for even electrodes for group A and odd electrodes for group B. The order in which the electrodes were presented was randomized. In addition, for each electrode, the presentation order of the three pulse shapes was also randomized. Then, thresholds were measured for even (group A) or for odd (group B) electrodes, also randomizing the electrode and pulse shape orders.

2. Speech recognition test and SMRT

3. Same as (1) for odd electrodes for group A and even electrodes for group B. Impedances were measured using the clinical fitting software (Soundwave v2.0, Advanced Bionics) at the beginning and at the end of the session.

2.7 Statistical analysis

The statistical analyses were performed using Matlab (MathWorks, Natick, MA), SPSS (PASW Statistics for Windows, v18.0. Chicago: SPSS Inc.) and MLwiN (Rasbash et al., (2009)).

First, we tested if one polarity was more efficient than the other by running a two sided-sign test with zero median on the polarity effect data.

Second, we examined the correlations between detection thresholds, EMDs and polarity effects both at the between-subject and within-subject levels. For the between-subjects analyses, the individual data were averaged across the electrode array, yielding one data point per subject. For the within-subject analyses, the data of all three measures (thresholds, EMD, polarity effect) were normalized by subtracting from each data point of a given subject the mean value across the array of this same subject. This removed the between-subject variance and allowed the data from all subjects to be pooled before calculating the correlation. (Bland and Altman, (1995); Carlyon et al., (2018)). Henceforth the term “normalized data” refers to this specific manipulation. To investigate the separate influence of EMD and polarity effect on detection thresholds, two analyses were carried out: (i) Partial correlations were calculated (SPSS) and (ii) a multilevel regression model was fitted to the detection threshold data (MLwiN).

Third, we correlated the mean polarity effect across the array of each subject (assumed to represent a global measure of neural health) to the performance on speech and SMRT tasks. The results of all correlations are presented by reporting the correlation coefficient, the degrees of freedom and the corresponding p-value (r, df, p, respectively).

3 Results

3.1 Detection thresholds

Figure 3 displays individual detection threshold measurements for the three pulse shapes, expressed in dB relative to 1 µA. Note that the vertical scale may be shifted between subjects to better visualize the differences in thresholds for the three pulse shapes but the range is identical. It is striking that the across-electrode patterns of thresholds are very subject-specific and that some of them exhibit large and highly localized peaks or troughs.

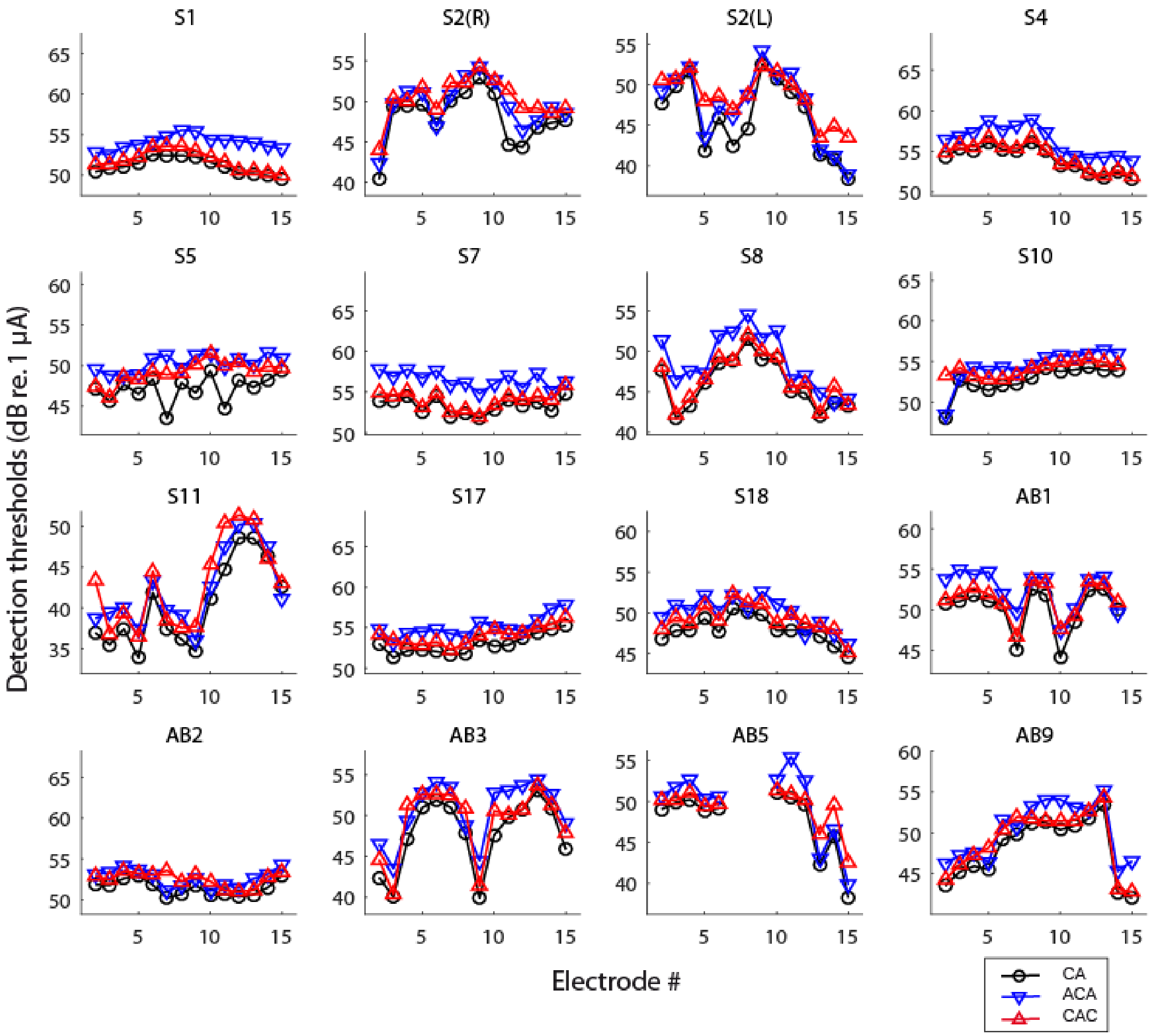

Figure 3: Detection thresholds (in decibels re. 1 µA) obtained for all pulse shapes (CA, ACA, and CAC) using pTP stimulation. Each panel is for one subject.

3.1.1 Polarity effect

CA-thresholds were always lower or equal to anodic (CAC) and cathodic (ACA) thresholds. This finding is predicted by the simple linear filter model of Carlyon et al., (2005) which accounts for the smoothing of the stimulus waveform at the level of the cell membrane. It may also relate to the fact that with CA pulses, both polarities are more likely to initiate action potentials (Coste and Pfingst, (1996); Undurraga et al., (2013)) and/or that triphasic pulses contain two phase reversals instead of one, which reduces the effect of the central phase (van Wieringen et al., (2008)). Polarity sensitivity was quantified by calculating the polarity effect, PE, defined as the difference in dB between cathodic and anodic thresholds. As a result, negative values of PE indicate that, for a given electrode, the cathodic threshold is lower than the anodic threshold. Figure 4 displays the individual across-electrode patterns of PE. Overall, out of 219 electrodes, 48 (22%) yielded negative PE (see figure 4). For each subject, we calculated the average of PE across the electrode array, referred to as $\overline{\mathrm{PE}}$ which can be considered as a global measure of polarity sensitivity. The average polarity effect ($\overline{\mathrm{PE}}$) was 0.87 dB and a sign test showed that across this group of CI users, the effect was more likely to be positive than negative (df = 15, p = 0.021). In other words, anodic thresholds were significantly more likely to be lower than cathodic thresholds for this group of CI users. Individual t-tests performed for each subject, on PE, yielded similar conclusions for ten out of sixteen ears tested. The polarity effect was not significantly different from zero for S2(L), S10, S11, AB2 and AB5. It was significantly negative for S2(R) (p=0.04).

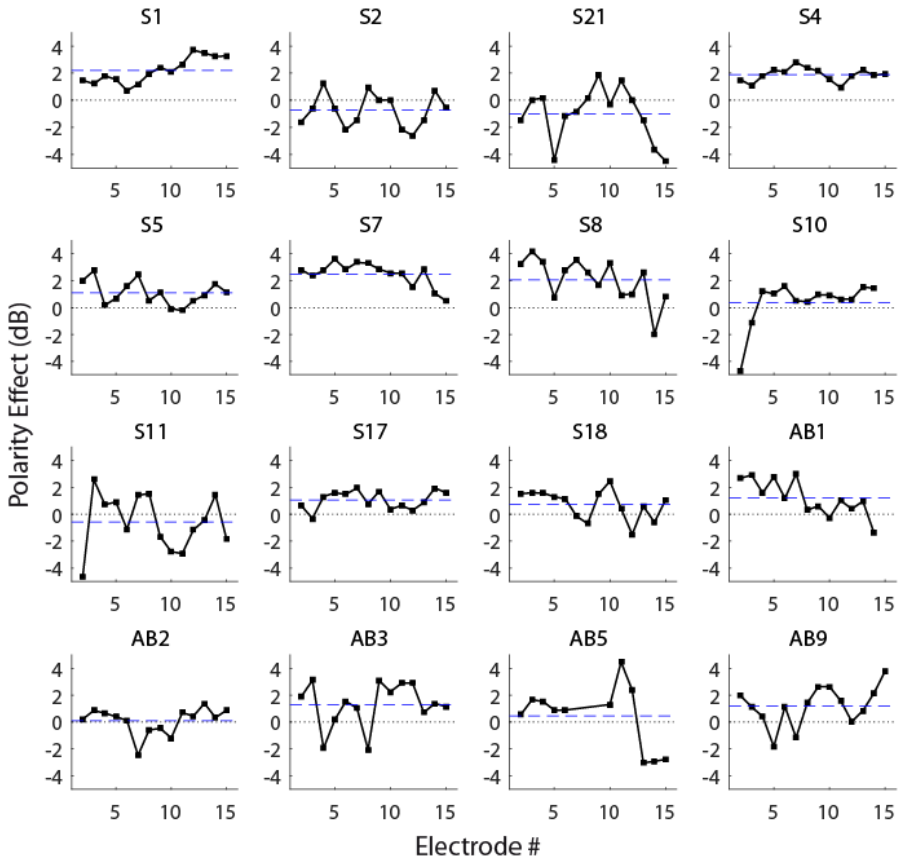

Figure 4: Across-electrode pattern of polarity effects obtained for each subject (Difference between cathodic and anodic thresholds in dB). Dotted lines indicate the 0 dB baseline. Dashed lines represent the mean PE.

If cathodic stimulation preferentially initiates action potentials at the level of the peripheral processes, the negative PE obtained for 48 of the electrodes tested may indicate that more peripheral processes are present in such cases. By extension, it may also imply that neural health is better near these electrodes.

The data were first averaged across the array for each subject. Pearson's correlations revealed a significant positive relationship between the mean thresholds with CA pulses and the mean polarity effect (r=0.50, df=14, p=0.047; Figure 5.A). However, this relationship might be partly driven by the left-most point on figure 5.A (+ symbol, corresponding to subject S11).

A weak but significant correlation was also observed at the within-subject level (ie. after removing the between-subject variance, Bland and Altman, (1995)) (r=0.19, df=201, p=0.006, Figure 5.B).

These results indicate that the polarity effect might explain a small part of the between- and within-subject variance in thresholds, and are broadly consistent with the findings of Carlyon et al., (2018), and Jahn and Arenberg (2019)

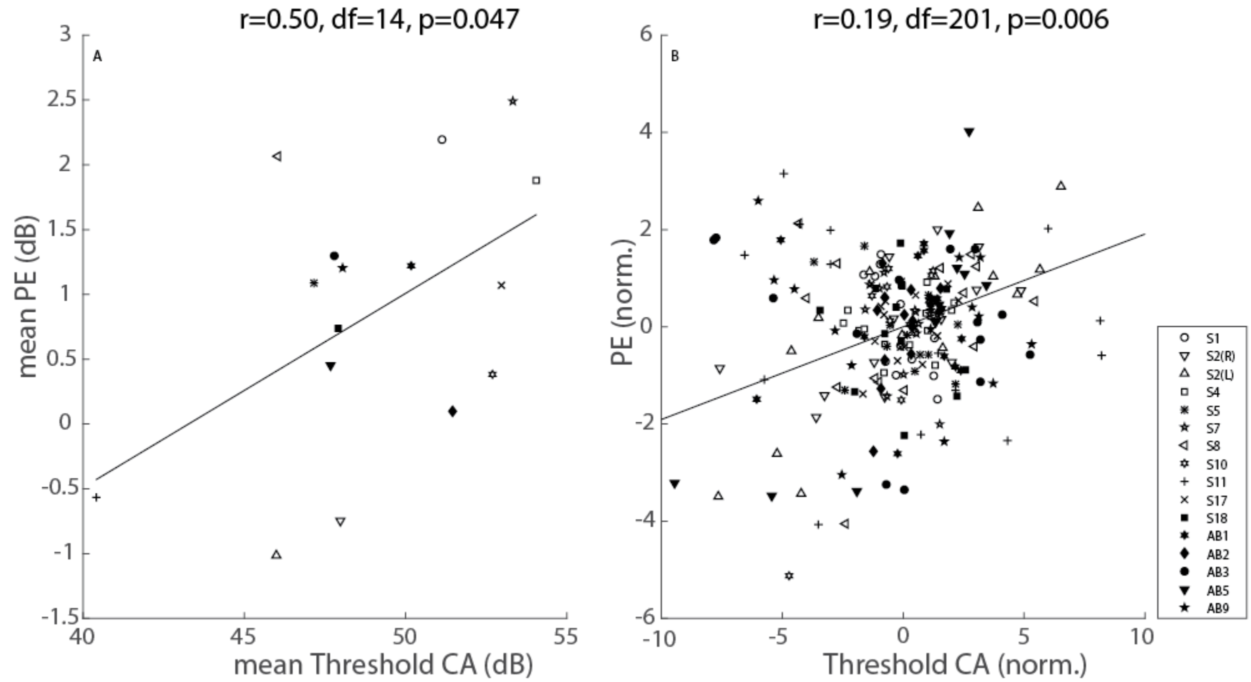

Figure 5: Panel A: Mean polarity effect (dB) as a function of the mean detection threshold (dB). Panel B: Normalized polarity effect as a function of the detection threshold (dB) measured with CA pulses, also normalized. Each symbol is for one subject

CT scans enabled the identification of irregular positions of some electrodes. S5 had his three or four most basal electrodes located inside the scala vestibuli. For S11, we spotted a tip fold-over on electrodes 1 and 2 (most apical). This subject also showed a large difference in polarity effect between electrodes 2 and 3, but it remains difficult to assess if this resulted from this abnormal positioning. As a matter of verification, the same analysis as in fig. 5 was carried out without these abnormally located electrodes. The within-subject correlation was still significant (r=0.20, df=197, p=0.005) but the between-subject correlation did not remain significant (r=0.48, df=14, p=0.052).

3.1.2 The effect of EMD

We assessed the reliability of EMD estimations using the methods described in Bland and Altman, (1999). Figure 6.A represents the EMDs reported by Observer 2 as a function of the EMDs reported by Observer 1 (r=0.83) . Figure 6.B illustrates the difference in EMDs between the two observers as a function of the average EMD from both observers, with dotted lines indicating the 95% confidence interval. Estimations within the confidence interval were averaged while the 6 electrodes falling beyond the confidence limits were not considered in the following statistical analyses.

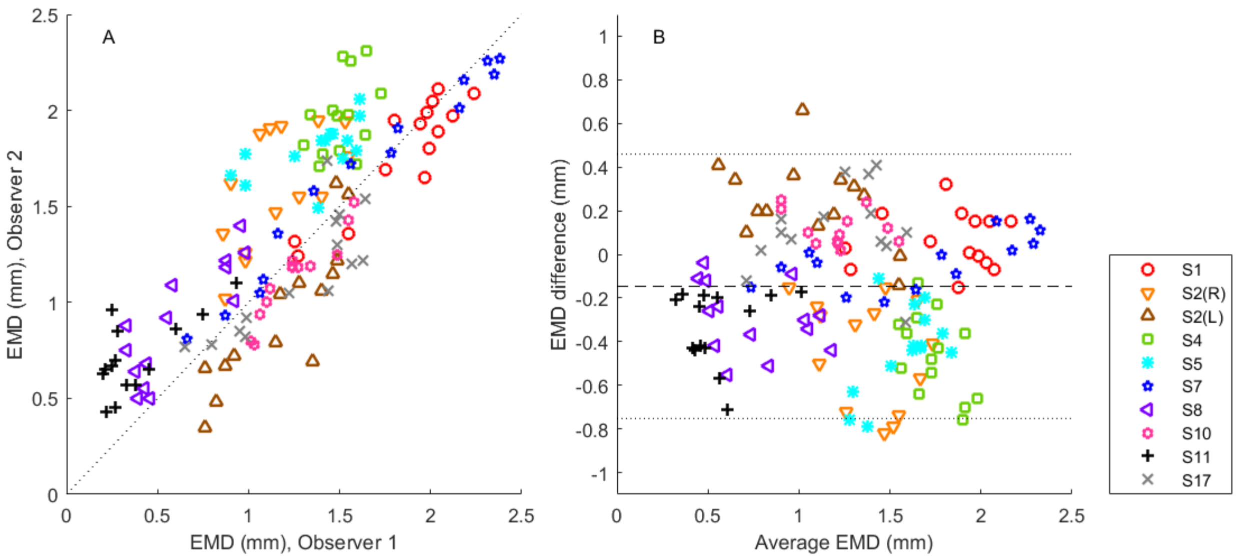

Figure 6: Panel A: EMD estimations from Observer 2 as a function of the EMD estimations from Observe 1 (mm). Dotted line represents the equality line. Panel B: EMD difference between the two observers as a function of the EMD averaged across the two observers. The dashed line represents the mean of the whole data set (-0.14 mm, the average absolute difference was 0.27 mm). The dotted lines represent the 95% confidence interval.

Figure 7 shows the individual EMD estimations as a function of the electrode number. Across the ten subjects for whom cone-beam CT scans were available, EMD estimates ranged between 0.32 and 2.33 mm, consistent with the observation of Jahn and Arenberg, (2019) for the same make of CIs.

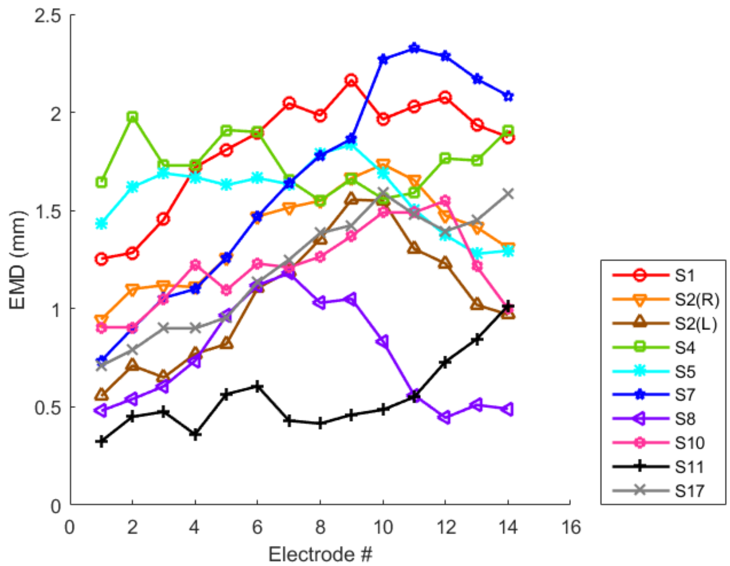

Figure 7: EMD estimations (mm) as a function of electrode number.

To analyze the between-subject variance in threshold, we calculated the mean threshold (across the array) and the mean EMD (across the array) for these 10 subjects. Figure 8 shows the variation of the mean threshold as a function of the mean EMD. Each symbol is for one subject. For all three pulse shapes, a significant positive correlation was found between EMDs and detection thresholds (df = 8, $p<0.05$; see figure 8). This model accounts for 52, 55 and 58% of the between-subject variance in thresholds for CA, ACA and CAC stimuli respectively. The EMD and the threshold patterns for each subject were then normalized by their mean value across the electrode array to pool the data from all subjects together and perform a within-subject correlation analysis. Figure 9 represents the normalized thresholds as a function of the EMD for the three pulse shapes. It shows that on average, only a small part of the within-subject variance in threshold can be explained by the EMD (average r=0.28, df =120, p<0.01). This poor relationship may be due to a small within-subject variability in EMD values. In other words, for any given subject, the EMD was relatively homogeneous across the electrode array but it could differ across

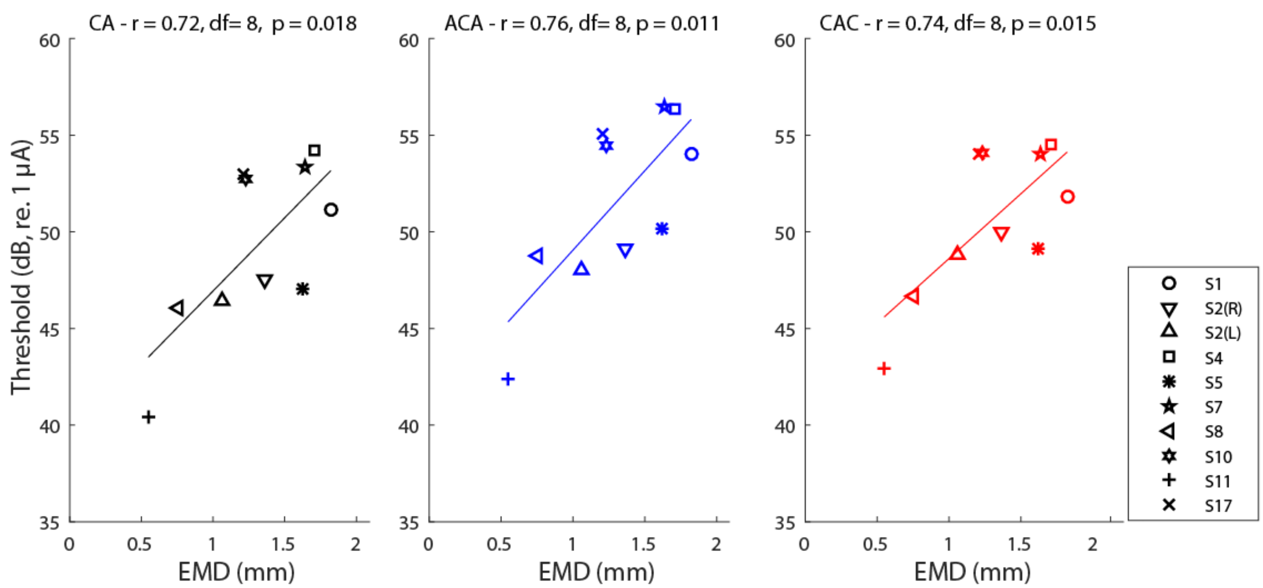

Figure 8: Mean detection threshold (dB) as a function of mean EMD (mm), averaged across the array. Each symbol is for one subject. Different panels illustrate the relationship for the three different pulse shapes CA, ACA and CAC.

subjects. For each subject, the difference in EMD between electrodes was smaller in our subject group (between 0.43 mm and 1.59 mm depending on the subject, 0.82 mm on average) than in Long et al., (2014), (0.75mm to 1.45mm, 1.20mm on average). This discrepancy will be discussed in section 4.

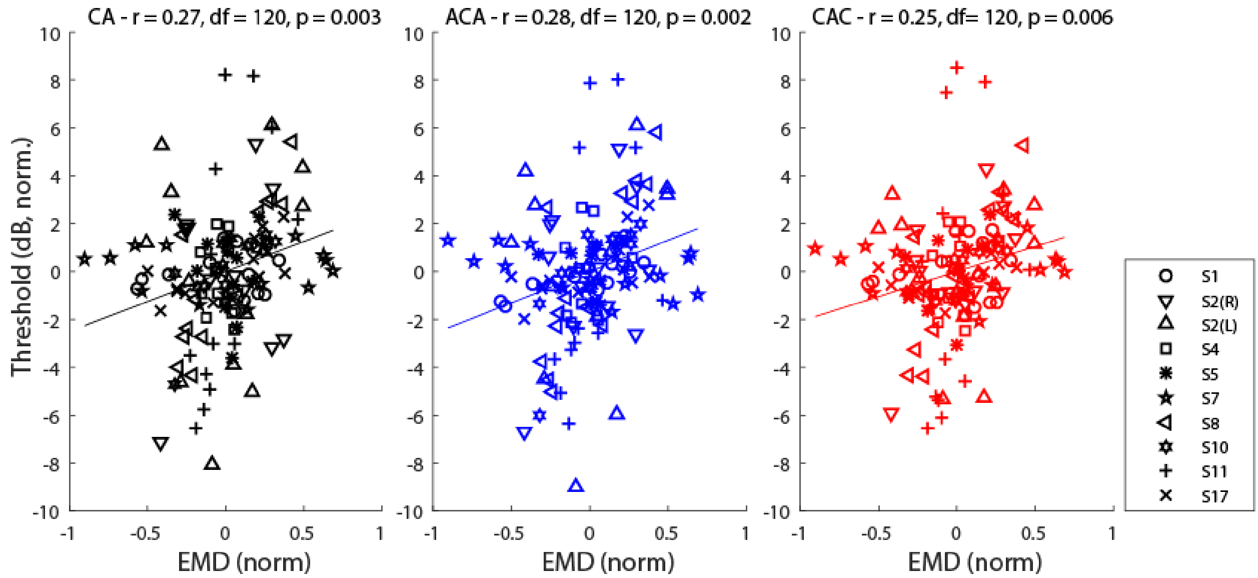

Figure 9: Normalized thresholds as a function of the normalized EMD. Each symbol is for one subject. Different panels illustrate the relationship for the three different pulse shapes CA, ACA and CAC.

3.1.3 Relationship between EMD, the polarity effect, and detection thresholds

The present findings suggest that both the EMD and PE have an influence on detection thresholds. However, the model study by Rattay, et al., (2001) suggested that polarity sensitivity may be influenced by the position of the electrode relative to the nerve fibers. It thus remains unclear whether the proportions of the threshold variance explained by these two parameters overlap. To investigate the combined contribution of EMD and PE on detection thresholds, partial correlation analyses were performed and the results are reported in Table 2. It indicates that detection thresholds correlate with both the EMDs and PEs and that each factor could only explain 6.5 and 4% of the variance respectively (when partialling out PE and the EMD, respectively).

It is also worth noting that no relationship was found between the EMDs and the PE when the detection thresholds were partialled out. We also fitted our data using a multilevel regression model which corroborated this finding (MLWin software, Rasbash et al., (2009), results not shown here). It therefore shows that both the EMD <u>and</u> PE contribute to explain some of the variance of the across-electrode threshold patterns.

3.2 Supra-threshold tasks

3.2.1 Speech recognition

Word recognition scores ranged from 20% to 68% with an average score of 43.2% for French speaking participants and 66.6% for English speaking participants. The test/retest reliability, expressed as the percentage of variation between the two lists, ranged between 0 and 24% (12% on average for French subjects and 7% for English subjects). Individual speech recognition scores are reported in Table 1. To be able to pool the speech recognition data from all participants, the logit of the speech scores were normalized by the mean value obtained in each group. Contrary to previous studies by Pfingst et al., (2004) and Long et al., (2014), in the present data, the within-subject variance in threshold was not correlated with the normalized logit of the speech recognition scores ($r = -0.24$, $df = 12$, $p = 0.399$).

Long et al., (2014) reported that neither mean threshold alone nor mean EMD alone predicted speech recognition scores. However, in their study, the root mean square error (RMSE) of the distance model was significantly correlated with speech intelligibility. As a result, they proposed the RMSE as a metric for the prediction of CI performance. For each of our subjects, the RMSE to the global distance model presented above was calculated. However, no such correlation was observed ($r=0.19$, $df=6$, $p=0.64$).

3.2.2 SMRT

The scores of the SMRT test carried out with all subjects ranged between 0.66 and 4.01 rpo with an average score of 1.84 rpo (see individual scores in table 1). Recently, O'Brien and Winn, (2017) reported that the transmission of spectral ripples through CI processors is subject to spectral aliasing and that additional cues may be used by the subjects to perform the task above a critical ripple density value. To circumvent this problem, the SMRT scores were winsorized with a maximum value of 2 rpo (corrected mean = 1.49 rpo).

It is worth noting that the outcomes of the speech recognition and SMRT tests were not correlated. This may relate to the inherent limitations of using this spectral ripple test with CIs as reported by O'Brien and Winn, (2017) or to the fact that speech recognition is more affected by individual factors such as experience with speech. As for speech scores, SMRT scores were not correlated to the RMSE (r=0.62, df =8, p=0.101). The within-subject variance in thresholds was not correlated to the SMRT scores (r = 0.44, df = 14, p = 0.085), however, one should mention that they were surprisingly positively correlated when considering the non-winsorized SMRT scores (r=0.62, df=14, p=0.010).

3.2.3 Comparison of polarity effect and performance on supra-threshold tasks

If, as suggested by the correlation between PE and detection threshold, PE relates to neural health, we would expect better performance in SMRT and speech recognition when PE is low. To evaluate this hypothesis, we consider the mean polarity effect averaged across the electrode array as previously defined. Figure 10 displays SMRT scores in rpo (Panel A), and normalized speech logit (Panel B) as a function of $\overline{\mathrm{PE}}$. We can note that SMRT scores show a significant negative relationship with $\overline{\mathrm{PE}}$ (r=-0.56, df=14, p=0.025) which corroborates our hypothesis that polarity sensitivity relates to neural health. Note that very similar correlations were obtained when using the non-winsorized SMRT scores (r=-0.55, df=14, p=0.026). In contrast, no significant relationship was observed between $\overline{\mathrm{PE}}$ and normalized speech recognition scores (r=0.42, df=12, p=0.136).

Besides, to assess the robustness of this global measure of neural health, the same correlation analysis was carried out for even and odd subsets of electrodes separately, which also yielded significant correlations between SMRT scores and the polarity effect (even electrode: r=-0.57, p=0.020; Odd electrodes: r=-0.52, p=0.041).

Here again these results are consistent with the hypothesis that PE relates to some aspects of neural health.

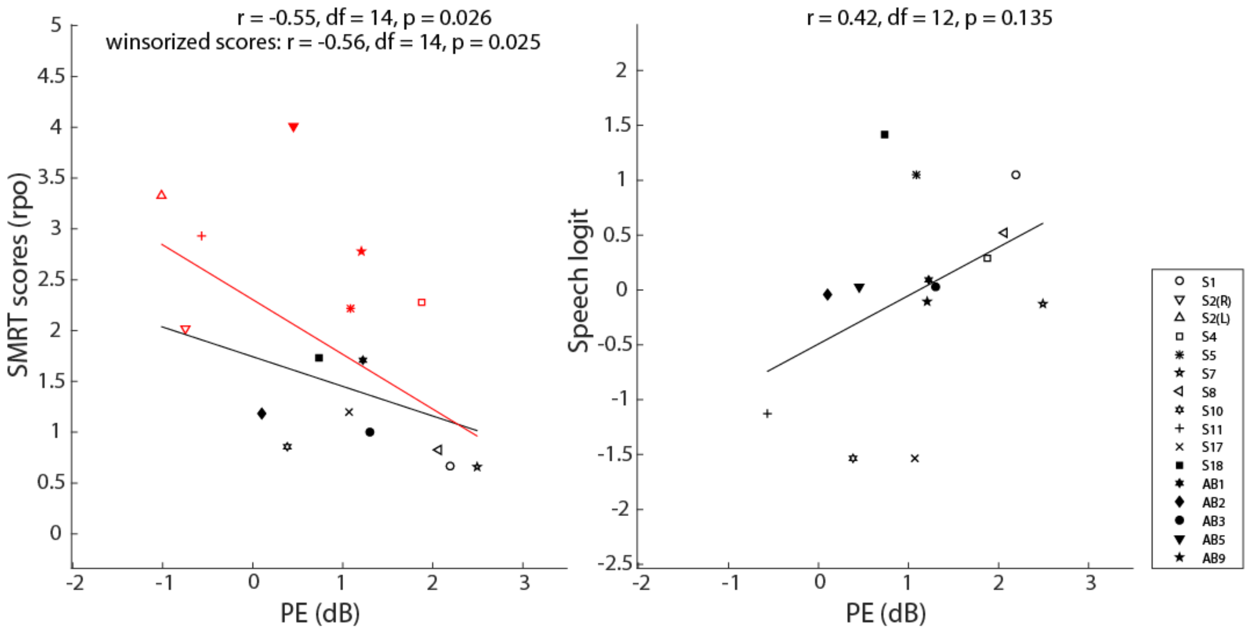

Figure 10: Panel A: SMRT scores (in ripples per octave) as a function of the difference between cathodic and anodic thresholds (in dB). Red symbols were winsorized for the correlation analysis. Panel B: Normalized logit of speech recognition scores as a function of the difference between cathodic and anodic thresholds (in dB).

4 Discussion and conclusion

We measured detection thresholds in CI users and tried to explain the across- and within-subject variability. In particular, we aimed to assess the influence of two potential factors on these detection thresholds: a measure of the distance between the electrodes and the nerve fibers, and a proposed psychophysical correlate of neural health. We tried to understand to what extent these factors relate to detection thresholds.

(1) Across-site variance in thresholds

Previous studies showed that speech performance is negatively correlated with the across-site variance in thresholds (Pfingst et al., (2004); Bierer, (2007); Long et al., (2014)). This measure of variance was thus proposed as a potential correlate of neural health. As in DeVries and Arenberg, (2018), speech test outcomes in the present experiment did not replicate those findings. Several factors may have influenced this lack of relationship. First, those earlier studies were conducted with a different device and different speech materials. Second, although Long et al., (2014) used a CNC word recognition test which is close to what was done in the present study, their subject group was also larger and more homogeneous than ours. In the present study, speech testing was carried out with the subjects' own processor meaning that the device settings/parameters differed across subjects. Furthermore, their experience with their device varied from 0.5 to 15 years. In contrast, in Long et al., (2014), all speech recognition tests were carried out 12 months post-activation and using the same external processor for all subjects, thereby providing the exact same stimulation strategy (Monopolar stimulation and ACE strategy). This might have reduced the number of subject-specific parameters that could influence speech recognition. Finally, the stimulation mode might play an important role since Long et al., (2014) found a significant relationship for PA and bipolar stimulation but not for tripolar and monopolar stimulation modes. In their study, monopolar stimulation yielded rather homogeneous across-electrode thresholds compared to PA (the within-subject variance in thresholds was 2.25 dB^2 on average for monopolar and 34.8 dB^2 for PA). In the present study, the average variance in thresholds using pTP stimulation was 8 dB^2. This relatively small variance might explain why it did not correlate with speech performance in the present study but did in their study with PA stimulation.

(2) Electrode-to-modiolar wall distance (EMD)

Consistent with several previous studies, we showed that the distance to the modiolar wall (i.e. near where the neurons lie) has an influence on detection threshold (Cohen et al., (2006); Long et al., (2014)). More specifically, we found that the distance model could explain 54% of the between-subject variance in thresholds but only 7% of the within-subject variance. As previously mentioned, this difference may result from the relatively small across-site variance in EMDs for our group of subjects.

Consistent with this observation, at the individual level, the so-called distance model was only significant for four of the ten subjects (S8, S10, S11 and S17). It is worth noting that in Long et al., (2014), a significant relationship was observed for seven of ten subjects with the phased-array electrode configuration (PA) and for only four of them with MP configuration. Another important factor might be that in their study all subjects were users of the Nucleus® perimodiolar electrode array while in the present study, only S2(L), S8 and S11 were implanted with an electrode array meant to be close to the modiolus (i.e. a HiFocus 1j with a positioner or a midscala electrode array).

Furthermore, we did not replicate the finding that speech scores correlate with the RMSE of the distance model.

Despite the difference in electrode configuration, one may wonder whether the acuracy of the EMD estimations might have affected the present results. Long et al., (2014) used a more advanced procedure for the estimation of the EMD. First, the resolution of our CT images was slightly poorer compared to Long et al., (2014) (125μm cubic voxels versus $100\mathrm{\mu m}$ in their study). In particular, the localization of the modiolar wall in the apical region was sometimes difficult due to a poor contrast and the presence of artifacts. Second, Long et al., (2014) had access to either pre-operative scans that were not contaminated by electrode artifacts, or to a scalable cochlear model, which was not our case. This resulted in a relatively large variability in the EMD estimations from both observers. While it was verified that the analysis conducted with each set of estimations yielded consitent results, it may be possible that this variability reduced the significance of the EMD as an explanatory factor for the variance in detection thresholds.

(3) Polarity sensitivity

Macherey et al., (2008) originally reported that human CI users consistently show a higher sensitivity to anodic stimulation at MCL. Other recent studies (Macherey et al., (2017); Carlyon et al., (2018); Goehring et al., (2019); Jahn and Arenberg, (2019)) reported that some subjects and/or electrodes may also exhibit a polarity sensitivity at threshold, which is reliable but can be in either direction. In the present study we analyzed a relatively large number of measurements which revealed a higher sensitivity to anodic stimulation for 78% of the tested electrodes at threshold.

Similar to the results of Jahn and Arenberg, (2019), who used the same methods for threshold measurements but using monopolar stimulation, no relationship was found between EMDs and the polarity effect. The partial correlations analysis suggests that both the EMD and PE contribute to the variance in thresholds.

From previous modeling studies (Rattay, et al., (2001); Resnick et al., (2018)), the difference between cathodic and anodic thresholds, PE is assumed to reflect the degree of degeneration or demyelination of the peripheral processes. In particular, high values of PE may relate to a place where peripheral processes cannot be stimulated or are degenerated. Interestingly, SMRT scores and $\overline{\mathrm{PE}}$ were negatively correlated. Even though the part of the variance in SMRT explained by $\overline{\mathrm{PE}}$ was small (31%), this result is consistent with this hypothesis.

(4) Perspectives

Even though we found that both the EMD and the polarity effect might contribute to explain this variance in threshold at both the between- and within-subject levels, the correlations were weak. This means that there may be other more central factors that are important and/or that polarity sensitivity only represents one aspect of neural health (e.g. survival of peripheral processes but not overall health).

Another limitation of the present result is that our analysis of the relationship between the performance on suprathreshold tasks and the polarity sensitivity only considered $\overline{\mathrm{PE}}$ which is averaged across the entire array and thus removes the information of the across-electrode differences in PE. It might thus be interesting to replicate this experiment with subsets of electrodes which exhibit little variation in PE to investigate the effect of polarity on performance in a within-subject analysis. Additional factors still need to be identified to better explain those results, these might for instance include the amount of fibrosis and/or ossification.

CT-scan analysis only enabled an estimation of the distance between the electrodes and the modiolar wall. A higher resolution might have enabled measurement not only of the EMD but also of the distance to the osseous spiral lamina (OSL). This distance may better represent the potential excitation site on the peripheral processes and also better relate to polarity sensitivity, as reported by Rattay, et al., (2001). In this case it would have been interesting to test the distance model on the one hand, between the EMD and anodic thresholds and, on the other hand, between the distance to the OSL and cathodic thresholds.

Although further investigation is required to strengthen the observation made in the present study, our results add some evidence that polarity sensitivity reflects some aspects of the electrode-neuron interface that have functional/perceptual implications (Carlyon et al., (2018); Hughes et al., (2018); Goehring et al, 2019). Being able to picture the places where healthy neurons lie may be beneficial for the optimization of stimulation strategies. In particular, current focusing and current steering techniques using multipolar strategies have been investigated in the past to create spatially selective virtual channels and thus improve spectral resolution (Berenstein et al., (2008); Bonham and Litvak, (2008)). While it was demonstrated that the locus of excitation might be slightly shifted by manipulating the amplitude of different electrodes, the benefits in terms of speech recognition were small or inconsistent across studies and/or subjects. The polarity effect might provide relevant information to further improve such strategies. It might also be used to select specific electrodes in order to target regions of the cochlea where the neural population is expected to be healthy.

Acknowledgments

We sincerely thank Alan Archer-Boyd, John Deeks, Debbie Vickers, Jean-Pierre Piron, Marielle Sicard, for their help with the data collection in Cambridge and in France and the CI participants for their work. This study was partly funded by Advanced Bionics.

Subjects	Duration of deafness prior to CI (years)	Etiology	CI use (years)	Age (years)	Deactivated electrodes	Speech scores (%)	SMRT scores (rpo)
S1	20	Unknown progressive	12	38	None	60	0.67
S2(R)	7	Unknown progressive	7	62	None	n/a	2.02
S2(L)	1	Unknown progressive	1	62	None	n/a	3.33
S4	10	Unknown progressive	13	52	None	47	2.28
S5	6	Usher syndrome	13	20	None	60	2.22
S7	24	Pendred syndrome	12	39	None	40	0.66
S8	2	Unknown progressive	15	87	None	51	0.83
S10	47	Ototoxicity following meningitis	12	61	E16	20	0.86
S11	34	Congenital	0.5	42	None	25	2.93
S17	10	Viral	11	63	None	20	1.20
S18	20	Possible ototoxicity	1.5	35	None	66	1.93
AB5	18	Otosclerosis	6	73	E8	67	4.01
AB1	n/a	n/a	7	71	E15	68	1.71
AB9	n/a	n/a	2	71	None	65	2.78
AB2	16	Acquired, possible	8	57	None	66	1.18

		ototoxicity					
AB3	33	Otosclerosis	8	70	None	67	1.00

Table 1: Subjects details. Subjects labelled with S- were tested in France, and those labelled with AB- were tested in the United Kingdom.

Variables	Control	r	df	p
Threshold, EMD	**PE**	0.25	117	0.006*
Threshold, PE	**EMD**	0.20	117	0.029*
EMD, PE	**Threshold**	0.06	117	0.516

Table 2: Partial correlations statistics.

Bibliography

Aronoff, and Landsberger. (2013). The development of a modified spectral ripple test. *The Journal of the Acoustical Society of America*, *134*(2), EL217-22. http://doi.org/10.1121/1.4813802

Berenstein, Mens, Mulder, and Vanpoucke. (2008). Current Steering and Current Focusing in Cochlear Implants : Comparison of Monopolar , Tripolar , and Virtual Channel Electrode Configurations. *Ear and Hearing*, *29*(2), 250–260.

Bierer. (2007). Threshold and channel interaction in cochlear implant users: evaluation of the tripolar electrode configuration. *The Journal of the Acoustical Society of America*, *121*(3), 1642–53. http://doi.org/10.1121/1.2436712

Bierer, Bierer, and Middlebrooks. (2011). Partial tripolar cochlear implant stimulation: Spread of excitation and forward masking in the inferior colliculus. *Hearing Research*, *4*(164), 134–142. http://doi.org/10.1126/scisignal.2001449.Engineering

Bierer, and Faulkner. (2010). Identifying cochlear implant channels with poor electrode-neuron interface: partial tripolar, single-channel thresholds and psychophysical tuning curves. *Ear and Hearing*, *4*(164), 247–258. http://doi.org/10.1126/scisignal.2001449.Engineering

Blamey, Artieres, Başkent, Bergeron, Beynon, Burke, … Lazard. (2013). Factors affecting auditory performance of postlinguistically deaf adults using cochlear implants: An update with 2251 patients. *Audiology and Neurotology*, *18*(1), 36–47. http://doi.org/10.1159/000343189

Bland, and Altman. (1995). Calculating correlation coefficients with repeated observations: Part 1 - correlation within subjects. *BMJ*, *310*, 446.

Bland, and Altman. (1999). Measuring agreement in method comparison studies with heteroscedastic measurements. *Statistical Methods in Medical Research*, *8*, 135–160. http://doi.org/10.1002/sim.5955

Bonham, and Litvak. (2008). Current Focusing and Steering. *Hearing Research*, *242*((1-2)), 141–153. http://doi.org/10.1016/j.heares.2008.03.006.

Bonnet, Frijns, Peeters, and Briaire. (2004). Speech recognition with a cochlear implant using triphasic charge-balanced pulses. *Acta Oto-Laryngologica*, *124*(4), 371–375. http://doi.org/10.1080/00016480410031084

Carlyon, Cosentino, Deeks, Parkinson, and Arenberg. (2018). Effect of Stimulus Polarity on Detection Thresholds in Cochlear Implant Users: Relationships with Average Threshold, Gap Detection, and Rate Discrimination. *JARO - Journal of the Association for Research in Otolaryngology*, *19*(5), 559–567. http://doi.org/10.1007/s10162-018-0677-5

Carlyon, Deeks, and Macherey. (2013). Polarity effects on place pitch and loudness for three cochlear-implant designs and at different cochlear sites. *The Journal of the Acoustical Society of America*, *134*(1), 503–509. http://doi.org/10.1121/1.4807900

Carlyon, van Wieringen, Deeks, Long, Lyzenga, and Wouters. (2005). Effect of inter-phase gap on the sensitivity of cochlear implant users to electrical stimulation. *Hearing Research*, *205*(1–2), 210–224. http://doi.org/10.1016/j.heares.2005.03.021

Cohen, Saunders, Knight, and Cowan. (2006). Psychophysical measures in patients fitted with Contour and straight Nucleus electrode arrays. *Hearing Research*, *212*(1–2), 160–75. http://doi.org/10.1016/j.heares.2005.11.005

Cosentino, Gaudrain, Deeks, and Carlyon. (2016). Multistage nonlinear optimization to recover neural activation patterns from evoked compound action potentials of cochlear implant users. *IEEE Transactions on Biomedical Engineering*, *63*(4), 833–840.

http://doi.org/10.1109/TBME.2015.2476373

Coste, and Pfingst. (1996). Stimulus features affecting psychophysical detection thresholds for electrical stimulation of the cochlea. III. Pulse polarity. *The Journal of the Acoustical Society of America*, *99*(5), 3099–3108. http://doi.org/10.1121/1.414796

DeVries, and Arenberg. (2018). Current Focusing to Reduce Channel Interaction for Distant Electrodes in Cochlear Implant Programs. *Trends in Hearing*, *22*, 1–18. http://doi.org/10.1177/2331216518813811

Eddington, Tierney, Noel, Hermann, Whearty, and Finley. (2004). *Speech processors for auditory prostheses. Ninth quarterly progress report, NIH contract N01-DC-2-1001,Neural Prosthesis Program, National Institutes of Health, Bethesda, MD*.

Escudé, James, Deguine, Cochard, Eter, and Fraysse. (2006). The size of the cochlea and predictions of insertion depth angles for cochlear implant electrodes. *Audiology and Neurotology*, *11*(SUPPL. 1), 27–33. http://doi.org/10.1159/000095611

Fayad, and Linthicum. (2006). Multichannel cochlear implants: Relation of histopathology to performance. *Laryngoscope*, *116*(8), 1310–1320. http://doi.org/10.1097/01.mlg.0000227176.09500.28

Garadat, Litovsky, Yu, and Zeng. (2010). Effects of simulated spectral holes on speech intelligibility and spatial release from masking under binaural and monaural listening. *The Journal of the Acoustical Society of America*, *127*(2), 977–989. http://doi.org/10.1121/1.3273897

Glueckert, Pfaller, Kinnefors, Rask-Andersen, and Schrott-Fischer. (2005). The human spiral ganglion: New insights into ultrastructure, survival rate and implications for cochlear implants. *Audiology and Neurotology*, *10*(5), 258–273. http://doi.org/10.1159/000086000

Goehring, Archer-Boyd, Deeks, Arenberg, and Carlyon. (2019). A Site-Selection Strategy Based on Polarity Sensitivity for Cochlear Implants: Effects on Spectro-Temporal Resolution and Speech Perception. *JARO - Journal of the Association for Research in Otolaryngology*, *20*(4), 431–448. http://doi.org/10.1007/s10162-019-00724-4

Hughes, Choi, and Glickman. (2018). What can stimulus polarity and interphase gap tell us about auditory nerve function in cochlear-implant recipients? *Hearing Research*, *359*, 50–63.

http://doi.org/10.1016/j.heares.2017.12.015

Jahn, and Arenberg. (2019). Evaluating Psychophysical Polarity Sensitivity as an Indirect Estimate of Neural Status in Cochlear Implant Listeners. *JARO - Journal of the Association for Research in Otolaryngology*. http://doi.org/10.1007/s10162-019-00718-2

Jolly, Spelman, and Clopton. (1996). Quadrupolar Stimulation for Cochlear Prostheses : Modeling and Experimental Data. *IEEE Transactions on Biomedical Engineering*, *43*(8), 857–865.

Kamakura, and Nadol. (2016). Correlation between word recognition score and intracochlear new bone and fibrous tissue after cochlear implantation in the human. *Hearing Research*. http://doi.org/10.1016/j.heares.2016.06.015

Khan, Handzel, Burgess, Damian, Eddington, and Nadol. (2005). Is Word Recognition Correlated With the Number of Surviving Spiral Ganglion Cells and Electrode Insertion Depth in Human Subjects With Cochlear Implants? *Laryngoscope*, *115*(April), 672–677.

Landsberger, Padilla, and Srinivasan. (2012). Reducing Current Spread using Current Focusing in Cochlear Implant Users. *Hearing Research*, *284*, 16–24. http://doi.org/10.1016/j.heares.2011.12.009.Reducing

Lawler, Yu, and Aronoff. (2017). HHS Public Access. *Ear and Hearing*, *38*(6), 760–766. http://doi.org/10.1097/AUD.0000000000000496

Linthicum, and Anderson. (1991). Cochlear Implantation of Totally Deaf Ears : Histologic Evaluation of Candidacy Cochlear Implantation of Totally Deaf Ears. *Acta Oto-Laryngologica*, *111*(2), 327–331. http://doi.org/10.3109/00016489109137395

Litvak. (2003). *BEDCS Bionic Ear Data Collection System. Version 1.16, user manual*.

Litvak, Spahr, and Emadi. (2007). Loudness growth observed under partially tripolar stimulation: model and data from cochlear implant listeners. *The Journal of the Acoustical Society of America*, *122*(2), 967–81. http://doi.org/10.1121/1.2749414

Long, Holden, McClelland, Parkinson, Shelton, Kelsall, and Smith. (2014). Examining the electro-neural interface of cochlear implant users using psychophysics, CT scans, and speech understanding. *Journal of the Association for Research in Otolaryngology*, *15*(2), 293–304. http://doi.org/10.1007/s10162-013-0437-5

Macherey, Carlyon, Chatron, and Roman. (2017). Effect of Pulse Polarity on Thresholds and on Non-monotonic Loudness Growth in Cochlear Implant Users. *JARO - Journal of the Association for Research in Otolaryngology*, *18*(3), 513–527. http://doi.org/10.1007/s10162-016-0614-4

Macherey, Carlyon, van Wieringen, Deeks, and Wouters. (2008). Higher sensitivity of human auditory nerve fibers to positive electrical currents. *Journal of the Association for Research in Otolaryngology : JARO*, *9*(2), 241–51. http://doi.org/10.1007/s10162-008-0112-4

Macherey, and Cazals. (2016). Effects of Pulse Shape and Polarity on Sensitivity to Cochlear Implant Stimulation : A Chronic Study in Guinea Pigs. *Advances in Expe*. http://doi.org/10.1007/978-3-319-25474-6

Macherey, van Wieringen, Carlyon, Deeks, and Wouters. (2006). Asymmetric pulses in cochlear implants: effects of pulse shape, polarity, and rate. *Journal of the Association for Research in Otolaryngology : JARO*, *7*(3), 253–66. http://doi.org/10.1007/s10162-006-0040-0

Mesnildrey, Macherey, Herzog, and Venail. (2019). Impedance measures for a better understanding of the electrical stimulation of the inner ear. *Journal of Neural Engineering*, *16*(1). http://doi.org/10.1088/1741-2552/aaecff

Micco, and Richter. (2006). Electrical resistivity measurements in the mammalian cochlea after neural degeneration. *The Laryngoscope*, *116*(8), 1334–1341. http://doi.org/10.1097/01.mlg.0000231828.37699.ab

Nadol, and Eddington. (2006). Histopathology of the Inner Ear Relevant to Cochlear Implantation. *Adv Otorhinolaryngol*, *64*, 31–39.

Nadol, Young, and Glynn. (1989). Survival of Spiral ganglion cells in profound Sensorineural hearing Loss : Implications for Cochlear Implantation. *Annals of Otology, Rhinology and Laryngology*, *98*, 411–416.

O’Brien, and Winn. (2017). Aliasing of spectral ripples through Speech, CI processors: A challenge to the interpretation of correlation with recognition scores. *Conference on Implantable Auditory Prostheses.*, *014309*(2007), 14309.

Pelliccia, Venail, Bonafé, Makeieff, Iannetti, Bartolomeo, and Mondain. (2014). Cochlea size variability and implications in clinical practice. *Acta Otorhinolaryngologica Italica : Organo*

Ufficiale Della Società Italiana Di Otorinolaringologia e Chirurgia Cervico-Facciale, *34*, 42–9. Retrieved from http://www.pubmedcentral.nih.gov/articlerender.fcgi?artid=3970226&tool=pmcentrez&rendertype=abstract

Pfingst, Colesa, Hembrador, Kang, Middlebrooks, Raphael, and Su. (2011). Detection of pulse trains in the electrically stimulated cochlea : Effects of cochlear health a). *Journal of the Acoustical Society of America*, *130*(December), 3954–3968. http://doi.org/10.1121/1.3651820

Pfingst, Xu, and Thompson. (2004). Across-Site Threshold Variation in Cochlear Implants: Relation to Speech Recognition. *Audiology and Neurotology*, *9*(6), 341–352.

Prado-Guitierrez, Fewster, Heasman, McKay, and Shepherd. (2007). Effect of interphase gap and pulse duration on electrically evoked potentials is correlated with auditory nerve survival. *Hearing Research*, *215*, 47–55.

Ramekers, Versnel, Strahl, Smeets, Klis, and Grolman. (2014). Auditory-nerve responses to varied inter-phase gap and phase duration of the electric pulse stimulus as predictors for neuronal degeneration. *JARO - Journal of the Association for Research in Otolaryngology*, *15*(2), 187–202. http://doi.org/10.1007/s10162-013-0440-x

Rasbash, Charlton, Browne, Healy, and Cameron. (2009). MLwiN Version 2.1. Centre for Multilevel Modelling, University of Bristol.

Rattay. (1999). The basic mechanism for the electrical stimulation of the nervous system. *Neuroscience*, *89*(2), 335–346.

Rattay, Leao, and Felix. (2001). A model of the electrically excited human cochlear neuron. II. Influence of the three-dimensional cochlear structure on neural excitability. *Hearing Research*, *153*(1–2), 64–79.

Rattay, Lutter, and Felix. (2001). A model of the electrically excited human cochlear neuronI. Contribution of neural substructures to the generation and propagation of spikes. *Hearing Research*, *153*(1–2), 43–63.

Resnick, O'Brien, and Rubinstein. (2018). Simulated auditory nerve axon demyelination alters sensitivity and response timing to extracellular stimulation. *Hearing Research*, *361*, 121–

137. http://doi.org/10.1016/j.heares.2018.01.014

Saunders, Cohen, Aschendorff, Shapiro, Knight, Stecker, … Cowan. (2002). Threshold, comfortable level and impedance changes as a function of electrode-modiolar distance. *Ear and Hearing*, *23*, 28S-40S. http://doi.org/10.1097/00003446-200202001-00004

Spelman, Clopton, and Pfingst. (1982). Tissue Impedance and Current Flow in the Implanted Ear Implications for the Cochlear Prosthesis. *Annals of Otology, Rhinology and Laryngology*, *suppl*(98), 3–8. Retrieved from http://www.ncbi.nlm.nih.gov/pubmed/?term=Tissue+Impedance+and+Current+Flow+in+the+Implanted+Ear+Implications+for+the+Cochlear+Prosthesis

Spoendlin. (1975). Retrograde degeneration of the cochlear nerve. *Acta Oto-Laryngologica*, *79*(3–6), 266–275. http://doi.org/10.3109/00016487509124683

Undurraga, Carlyon, Wouters, and van Wieringen. (2013). The Polarity Sensitivity of the Electrically Stimulated Human Auditory Nerve Measured at the Level of the Brainstem. *JARO - Journal of the Association for Research in Otolaryngology*, *14*, 359–377. http://doi.org/10.1007/s10162-013-0377-0

van der Marel, Briaire, Verbist, Muurling, and Frijns. (2015). The Influence of Cochlear Implant Electrode Position on Performance. *Audiology and Neurotology*, *20*(3), 202–211. http://doi.org/10.1159/000377616

van Wieringen, Macherey, Carlyon, Deeks, and Wouters. (2008). Alternative pulse shapes in electrical hearing. *Hearing Research*, *242*(1–2), 154–163. http://doi.org/10.1016/j.heares.2008.03.005

Vanpoucke, Zarowski, and Peeters. (2004). Identification of the impedance model of an implanted cochlear prosthesis from intracochlear potential measurements. *IEEE Transactions on Bio-Medical Engineering*, *51*(12), 2174–83. http://doi.org/10.1109/TBME.2004.836518

Venail, Mathiolon, Menjot de Champfleur, Piron, Sicard, Villemus, … Uziel. (2015). Effects of Electrode Array Length on Frequency-Place Mismatch and Speech Perception with Cochlear Implants. *Audiology and Neurotology*, 102–111. http://doi.org/10.1159/000369333

Won, Drennan, and Rubinstein. (2007). Spectral-Ripple Resolution Correlates with Speech

Reception in Noise in Cochlear Implant Users. *JARO - Journal of the Association for Research in Otolaryngology*, *8*, 384–392. http://doi.org/10.1007/s10162-007-0085-8

Zhou, and Pfingst. (2014). Relationship between multipulse integration and speech recognition with cochlear implants. *Journal of the Acoustical Society of America*, *136*(September), 1257–1268. http://doi.org/10.1121/1.4890640

Title:

Polarity sensitivity as a potential correlate of neural degeneration in cochlear implant users[1].

Authors:

- Quentin Mesnildrey[a] (corresponding author, ORCID: 0000-0003-2149-3599);
- Frédéric Venail[b];
- Robert P. Carlyon[c];
- Olivier Macherey[a].

Affiliations:

a- Aix-Marseille Univ., Centrale Marseille, CNRS, LMA, Marseille, France.

b- ENT Department and University Hospital, Montpellier, France.

c- Medical Research Council, Cognition and Brain Sciences Unit, University of Cambridge, United Kingdom.

Key words:

cochlear implant, polarity, neural health ~~survival~~, computed tomography scans

Abstract

Cochlear implant (CI) performance varies dramatically between subjects. Although the causes of this variability remain unclear, the electrode-neuron interface is thought to play an important role. Here we evaluate the contribution of two parameters of this interface on the perception of CI listeners: the electrode-to-modiolar wall distance (EMD), estimated from cone-beam computed tomography (CT) scans, and a measure of neural health. ~~the state of neural degeneration~~. ~~Unfortunately~~ Since there is no objective way to quantify neural health ~~survival~~ in

[1] Part of this work was presented at the Conference on Implantable Auditory Prostheses in Lake Tahoe, California, 2017

CI users~~. Therefore,~~ we measure ~~investigate~~ ~~whether~~ stimulus polarity sensitivity, which is assumed to be related to neural degeneration, and investigate whether it also correlates with subjects' performance in speech recognition and spectro-temporal modulation detection tasks. Detection thresholds were measured in fifteen CI users (sixteen ears) for partial-tripolar triphasic pulses having an anodic or a cathodic central phase. The polarity effect was defined as the difference in threshold between cathodic and anodic stimuli. Our results show that both the EMD and the polarity effect correlate with detection thresholds, both across and within subjects, although the within-subject correlations were weak. Furthermore, the mean polarity effect, averaged across all electrodes for each subject was negatively correlated with performance on a spectro-temporal modulation detection task. In other words, lower cathodic thresholds were associated with better spectro-temporal modulation detection performance, which is also consistent with polarity sensitivity being a marker of neural degeneration. Implications for the design of future subject-specific fitting strategies are discussed.

Number of tables: 2

Number of figures: 10

1 Introduction

Several studies have shown that the variability in performance of cochlear implant (CI) users is at least partly due to differences in the electrode-neuron interface (Bierer and Faulkner, (2010); Cosentino et al., (2016); Garadat et al., (2010)). A conceptual model of this interface involves (1) the electrode position, (2) the current path from the electrode to the neurons and (3) the distribution of the neural population. While (1) and (2) can respectively be investigated by analyzing CT images (Saunders et al., (2002); Cohen et al., (2006); Long et al., (2014); van der Marel et al., (2015); Venail et al., (2015)) and by performing electrical measurements (Spelman et al., (1982); Vanpoucke et al., (2004); Micco and Richter, (2006); Mesnildrey et al., (2019)) assessing neural health ~~survival~~ remains a challenge.

Studies counting the remaining cells in cadaver cochleas showed the complexity of predicting neural health ~~survival~~ in CI patients, because the speed of neural degeneration depends on numerous factors such as the duration and etiology of deafness (Nadol et al., (1989); Linthicum and Anderson, (1991); Glueckert et al., (2005)). In addition, and rather surprisingly, studies that examined the correlation between the number of remaining nerve fibers and speech performance have yielded inconsistent results (Khan et al., (2005); Fayad and Linthicum, (2006); Nadol and Eddington, (2006); Kamakura and Nadol, (2016)).

Since it is currently not possible to objectively quantify neural survival in CI users, several studies have tried to identify psychophysical or electrophysiological correlates. Pfingst et al., (2004) and Long et al., (2014) reported correlations between the within-subject variance in threshold across the electrode array and speech performance. They argued that a large threshold variance across the array may reflect the presence of neural dead regions, which would negatively impact speech perception. Zhou and Pfingst, (2014) measured the effect of electrical pulse rate on threshold, termed multipulse integration, in human CI users. They proposed, based on similar experiments in animals (Pfingst et al., (2011)), that the decrease in threshold associated with a doubling of the pulse rate could be a psychophysical correlate of neural health ~~survival~~. Consistent with this hypothesis, they reported that the amplitude of the multipulse integration was positively correlated with consonant recognition in noise.

Animal studies by Prado-Guitierrez et al., 2007 and Ramekers et al., 2014 examined the effect of two parameters - the inter-phase gap and the phase duration - on the amplitude of the electrically-evoked compound action potential (eCAP). Prado-Guitierrez et al., (2007) reported that the increase in eCAP amplitude as a function of both the inter-phase gap and the phase duration was larger in healthy cochleas. The same relationship was found in Ramekers et al., (2014) for the inter-phase gap only.

A modelling study by Rattay, (1999) investigated the response of single nerve fibers to electrical stimulation. They predicted that the site of excitation along the nerve fibers should depend on stimulus polarity. In particular, they showed that cathodic stimulation tends to yield longer latencies than anodic stimulation for it is more likely to initiate action potentials at the peripheral processes. Similar observations were made by Rattay et al., (2001) and more recently by Resnick et al., (2018). Another important result from Resnick et al., (2018) is that a partial demyelination of peripheral processes reduces its excitability and yields an incease in threshold for cathodic but not for anodic stimulation. Polarity sensitivity may thus directly relate to the state of degeneration or demyelination of the peripheral processes. Since neural degeneration is retrograde by nature (Spoendlin, (1975)), it is also possible that the regions with a lot of peripheral degeneration are also regions where the number of surviving neurons is low. As a result, one may assume polarity sensitivity to relate to the local state of the neural population. More specifically, a relatively higher sensitivity to anodic stimulation compared to cathodic stimulation may reflect a site with high neural degeneration.

Polarity sensitivity can be assessed in human CI users by means of asymmetric pulse shapes, such as pseudomonophasic or triphasic pulses (Figure 1, Bonnet et al., (2004); Eddington et al., (2004); Macherey et al., (2008), (2006)). Unlike clinical symmetric biphasic pulses, such asymmetric pulse shapes can induce a domination of one polarity over the other, while maintaining electrical charge balance (Carlyon et al., (2013)). Macherey et al., (2017) demonstrated that polarity sensitivity at detection threshold can differ across human CI users, or across electrodes for a given subject. These differences have also been assumed to relate to the state of neural degeneration or demyelination of the peripheral processes.

Based on these studies, measuring polarity sensitivity across the electrode array has recently been proposed as an estimate of neural health ~~survival~~ along the cochlea (Carlyon et al., (2018); Hughes et al., (2018)).

Here we measure the polarity effect, defined as the difference in threshold between cathodic (Fig. 1.B) and anodic (Fig. 1.C) stimulation. Our first aim is to investigate how it relates to overall sensitivity across the electrode array (detection threshold). Furthermore, computational modeling by Rattay et al., (2001) predicts that the polarity effect may also depend on the position of the electrode in the scala tympani. Given that detection thresholds have also been shown to depend on the electrode-to-modiolar wall distance (EMD), we estimate this distance in a subset of our subjects from whom scans are available. This allows us to study the separate contributions of the EMD and of the polarity effect on overall sensitivity. Finally, assuming the polarity effect is a correlate of neural health ~~survival~~, we would expect it to be related to overall performance on suprathreshold tasks. A second aim of the present study is to correlate the polarity effect with performance on speech perception tasks and/or to measures of spectro-temporal modulation discrimination (Won et al., (2007); Aronoff and Landsberger, (2013)). We hypothesize that a large positive polarity effect reveals poor neural health ~~survival~~ while a negative polarity effect reveals good neural health ~~survival~~. We would thus expect the performance on suprathreshold tasks to be negatively correlated with the polarity effect.

Another measure of interest concerns the variation in threshold across electrodes. Long et al., (2014) measured detection thresholds, EMD and speech recognition in a group of CI users implanted with an experimental version of the device manufactured by Cochlear Corporation. For seven of their ten subjects, detection thresholds were positively correlated with the EMDs, referred to as the distance model. Interestingly, speech recognition scores were correlated with the residuals of the distance model, meaning that when the distance could not explain the variation in threshold across electrodes, speech performance tended to be poorer. They hypothesized that this might reflect the irregularity of neural health ~~survival~~ across the electrode array. Here we also aim to replicate this experiment with a different CI group implanted with a device from a different manufacturer.

2 Methods

2.1 Subjects

Experiments were conducted both in Marseille (France) and in Cambridge (United Kingdom) with a total of 15 adult CI users (16 ears) whose details are reported in Table 1. Ten subjects (11 ears) were tested in Marseille and five were tested in Cambridge. All subjects were implanted with a CII/HiRes 90k device manufactured by Advanced Bionics. Their electrode array was the HiFocus 1j except for subjects S2(L) and AB9 who had the MidScala electrode. The labels S2(L) and S2(R) refer to the left and right ears of the same bilaterally-implanted subject. In the following, the data corresponding to each ear were treated as separate data sets. Subjects were paid for their participation. All experiments were approved by the ethics committees (Marseille: Eudract 2012-A00438-35; Cambridge: 00/327).

2.2 Detection thresholds

Detection thresholds were measured for all subjects using the Bionic Ear Data Collection System

(BEDCS, Advanced Bionics, Litvak, (2003)) and custom Matlab interfaces.

Stimuli

Electrical stimuli were 300-ms pulse trains presented at a rate of 100 pulses per second. Three pulse shapes were used (Figure 1): Cathodic-first symmetric biphasic pulses (CA), triphasic pulses with a cathodic central phase (ACA) and triphasic with an anodic central phase (CAC). The triphasic pulse shapes consisted of a central phase of a given polarity and amplitude, preceded and followed by opposite-polarity phases of the same duration and half the amplitude so as to maintain charge-balancing. ACA and CAC pulses were intended to enhance the influence of the cathodic and anodic phase respectively (Eddington et al., (2004); Carlyon et al., (2013); Macherey and Cazals, (2016)). Henceforth, ACA and CAC thresholds are referred to as cathodic and anodic thresholds, respectively. For all pulse shapes, the duration of each phase was 97 µs.

Stimuli were presented in partial tripolar (pTP) configuration with 75% of the current returning to the flanking electrodes and 25% to the ground (i.e. $\sigma = 0.75$, Jolly et al., (1996); Litvak et al., (2007)). Forward-masking experiments have provided evidence that pTP may produce a more spatially-focused stimulation than MP (Bierer et al., (2011); Landsberger et al., (2012)). We thus expected detection thresholds to reflect the responsiveness of restricted portions of the auditory nerve.

In pTP stimulation mode, the most apical and most basal electrodes cannot be stimulated because they do not have two neighboring electrodes, thereby limiting the maximum number of available tripolar channels to 14 (central electrodes ranging from E2 to E15). Any electrode deactivated in the patients' clinical maps (see table 1) was not tested (neither as central electrodes nor as flanking electrodes).

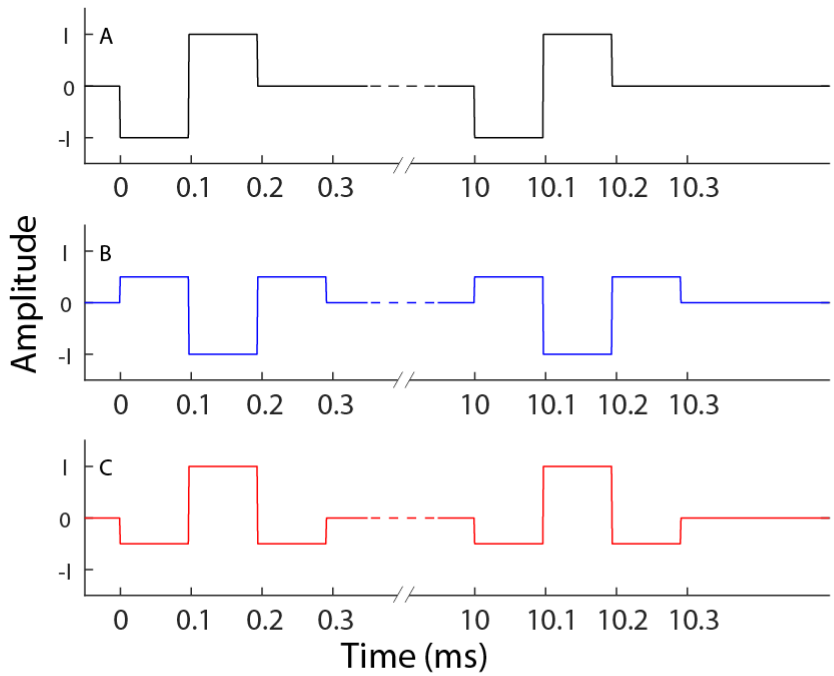

Figure 1: Electrical pulse shapes used for threshold measurements. Panel A: cathodic-first biphasic pulses (CA). Panel B: triphasic cathodic pulses (ACA). Panel C: triphasic anodic pulses (CAC).

Procedure

For most subjects the number of conditions was 42 ({14 electrodes}×{3 pulse shapes}) but this was reduced when an electrode was deactivated in the subject's clinical map (Table 1). Subject AB5, for whom an electrode in the middle of the array was deactivated, was tested on 11 electrodes (total of 33 conditions). The duration of a session only enabled one measure per condition. The thresholds for even and odd electrodes were measured separately yielding two blocks of 7 electrodes and 21 testing conditions. This procedure was chosen, first, to introduce a break approximately half-way through the session and, second, to be able to run independent analysis for both sets of electrodes, which will provide a control on the reliability of the measures. For each subset, one electrode was randomly selected and the three pulse shapes were tested successively, also in a randomized order. The most comfortable level (MCL) was then estimated for each specific condition.

Subjects were asked to report the perceived loudness using a loudness chart ranging from 0 to 10, where 1 corresponds to the quietest just noticeable sound, 6 to the MCL and 10 to sounds that are too loud. The stimulation level was manually increased with an amplitude step of 1 dB starting at a subthreshold level. Typically, when the loudness reached level 2, the amplitude step was reduced to 0.5 dB up to loudness level 4 and then further reduced to 0.2 dB until the MCL was reached. Before each stimulation, it was checked that the current level did not exceed the compliance limit (7 Volts) of the device. If the compliance limit was reached before the MCL, the procedure was stopped and the maximum current level allowed was recorded.

After measuring the MCLs for all 21 conditions, detection thresholds were obtained for each condition using a one-up/one-down procedure. A single 300-ms stimulus was played at an initial level corresponding to 90% of the MCL (or 90% of the maximum level below the compliance limit). Subjects were asked to press the space bar of a computer keyboard when they heard a sound. If a percept was reported within a three-second time window, a lower-amplitude stimulus was played after a random delay ranging between two and three seconds. In the absence of a response after three seconds, a higher-amplitude stimulus was played after a shorter random delay (between 0.1 s and 0.6 s). As a result, with or without a response, the duration between two consecutive stimuli varied between two and six seconds. This timing was chosen after a pilot experiment because it appeared to be a good compromise for a relatively fast procedure while giving the subjects enough time to respond.

Note that, although thresholds obtained with this procedure may have been affected by differences in response criterion between subjects, this would not be expected to influence the difference between anodic and cathodic thresholds.

During this automatic procedure, the incremental/decremental step in level was ± 0.5 dB until the first reversal and ± 0.2 dB afterwards. The procedure stopped after eight reversals and each threshold was calculated as the average of the last six reversals.

2.3 Speech recognition

Depending on the testing location, speech recognition was measured in a sound-insulated booth or in an anechoic chamber using the subjects’ own speech processor and clinical map. Two lists of single words (i.e. 100 words in total) from the French (N=9) or British (N=5) versions of the Phonetically Balanced Kindergarten corpus (PBK, Haskins, 1949) were presented to each individual listener. S2 is an American English speaker and thus did not participate in this task. Acoustic stimuli were played in free field through a Fostex 6301B loudspeaker without masking noise. Subjects sat one meter away from the loudspeaker, where the sound pressure level was adjusted to 65 dB. They were asked to repeat each word they heard. Correct and incorrect responses were scored by an experimenter sitting next to the subject and no feedback was provided.

2.4 Spectro-temporally Modulated Ripple Test, (SMRT)

In this study, apart from different native languages, CI users also had a wide variability of experience with their device (see table 1). CI experience varied from 0.5 to 15 years and some of the subjects were prelingually deaf (S5 and S10). To limit the effect of CI experience (Blamey et al., (2013)) and of native language, a spectro-temporally modulated ripple test (SMRT, Aronoff and Landsberger, (2013)) which reflects the ability of subjects to receive and integrate spectro-temporal cues, was also carried out with all 15 subjects. This test and similar ones have been shown to correlate with speech recognition performance in CI users (Won et al., (2007); Lawler et al., (2017)).

The SMRT test is implemented as a 3-interval, 3 alternative forced choice adaptive procedure. Two of the intervals contain a reference stimulus and one contains the target stimulus. The reference has a constant density of 20 ripples per octave (rpo) while the target has an initial density of 0.5 rpo. A one-up/one-down adaptive procedure runs with steps of 0.2 rpo until the subject cannot differentiate the target from the reference. Thresholds are given based on the average of the last six reversals and are expressed in number of rpo. For this test, subjects also used their own processor and clinical map. Stimuli were presented in the same experimental conditions as in the speech recognition experiment (i.e. free field acoustic stimulation at a level of 65 dB SPL). After one run of training with feedback, two additional test runs were carried out without feedback and the outcome measure is given as the average of these two test runs.

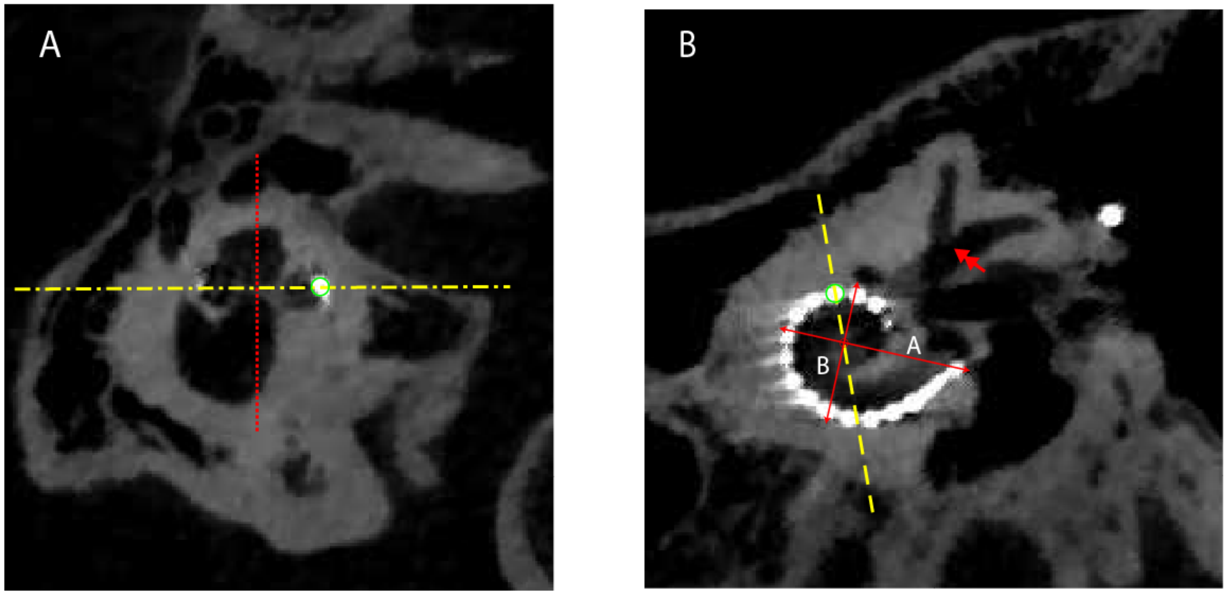

Figure 2: Panel A: vertical section view of the implanted cochlea. The red dotted line represents the modiolar axis, the yellow dash-dotted line represents the horizontal section plane corresponding to panel B. Panel B: Horizontal section of the basal turn of the cochlea. Dashed line: vertical section plane corresponding to panel A. Double arrow head: superior and lateral semicircular canals. The green circle in both panels mark the same electrode

2.5 Electrode-to-modiolar wall distance

The CT scans (Cone beam 5G Newtom, $125\mu m \times 125\mu m \times 125\mu m$ voxels) from 10 ears (S1-2(R)-2(L)-4-5-7-8-10-11-17), were analyzed using the Onis Pro software (v2.5 DigitalCore®, Co. LTD) in order to estimate the electrode-to-modiolar wall distance, (EMD).

CT images were oriented using the method described in Escudé et al., (2006). The 3D manipulating tool was used in order to visualize the basal turn of the cochlea, the vestibule and the anterior branches of the lateral and superior semicircular canals. We marked the largest distance from the round window through the modiolus to the lateral wall (distance A on Fig. 2), and the largest distance perpendicular to A (distance B on Fig. 2). The modiolar axis was defined as the intersection of A and B. In the following, the view perpendicular to the modiolar axis (Fig. 2B) is referred to as the horizontal view and the mid-modiolar sections are referred to as vertical views (Fig. 2A).

As in Escudé et al., (2006) and Pelliccia et al., (2014), the image orientation was validated using both the horizontal and vertical views. Note that the image orientation was made by considering the cochlear geometry rather than the electrode array. The image contrast was then adjusted to offer the best representation of both the modiolar wall and the electrode. Here again the position of the modiolar wall located using one view was validated using orthogonal views.

The position of each electrode was assumed to be at the center of the artifact. Prior to the EMD measurements, the CT images were rotated around the modiolar axis in order to visualize the specific electrode on both horizontal and vertical section views. The green circles in Fig. 2 identify the same electrode in both the horizontal and vertical views.

The EMD was then measured using the software measuring tool as the radial distance from the electrode to the modiolar wall (as revealed by a higher contrast). Again EMD estimations were validated using both horizontal and vertical views. Two independent sets of EMD estimations were made by two observers. Since, in humans, spiral ganglion cells (SGCs) are clustered in Rosenthal's canal, this measurement gives a first approximation of the distance between the electrodes and the SGCs.

2.6 Testing Session

Threshold measurements, speech recognition test and SMRT were carried out in the same session lasting approximately three hours. The subjects were divided in two groups (A and B). Group A started with measurements on the even electrodes while group B started with measurements on the odd electrodes. Each session was organized as follows:

1. MCL estimation for even electrodes for group A and odd electrodes for group B. The order in which the electrodes were presented was randomized. In addition, for each electrode, the presentation order of the three pulse shapes was also randomized. Then, thresholds were measured for even (group A) or for odd (group B) electrodes, also randomizing the electrode and pulse shape orders.

2. Speech recognition test and SMRT

3. Same as (1) for odd electrodes for group A and even electrodes for group B. Impedances were measured using the clinical fitting software (Soundwave v2.0, Advanced Bionics) at the beginning and at the end of the session.

2.7 Statistical analysis

The statistical analyses were performed using Matlab (MathWorks, Natick, MA), SPSS (PASW Statistics for Windows, v18.0. Chicago: SPSS Inc.) and MLwiN (Rasbash et al., (2009)).

First, we tested if one polarity was more efficient than the other by running a two sided-sign test with zero median on the polarity effect data.

Second, we examined the correlations between detection thresholds, EMDs and polarity effects both at the between-subject and within-subject levels. For the between-subjects analyses, the individual data were averaged across the electrode array, yielding one data point per subject. For the within-subject analyses, the data of all three measures (thresholds, EMD, polarity effect) were normalized by subtracting from each data point of a given subject the mean value across the array of this same subject. This removed the between-subject variance and allowed the data from all subjects to be pooled before calculating the correlation. (Bland and Altman, (1995); Carlyon et al., (2018)). Henceforth the term "normalized data" refers to this specific manipulation. To investigate the separate influence of EMD and polarity effect on detection thresholds, two analyses were carried out: (i) Partial correlations were calculated (SPSS) and (ii) a multilevel regression model was fitted to the detection threshold data (MLwiN).

Third, we correlated the mean polarity effect across the array of each subject (assumed to represent a global measure of neural health ~~survival~~) to the performance on speech and SMRT tasks. The results of all correlations are presented by reporting the correlation coefficient, the degrees of freedom and the corresponding p-value (r, df, p, respectively).

3 Results

3.1 Detection thresholds

Figure 3 displays individual detection threshold measurements for the three pulse shapes, expressed in dB relative to 1 µA. Note that the vertical scale may be shifted between subjects to better visualize the differences in thresholds for the three pulse shapes but the range is identical. It is striking that the across-electrode patterns of thresholds are very subject-specific and that some of them exhibit large and highly localized peaks or troughs.

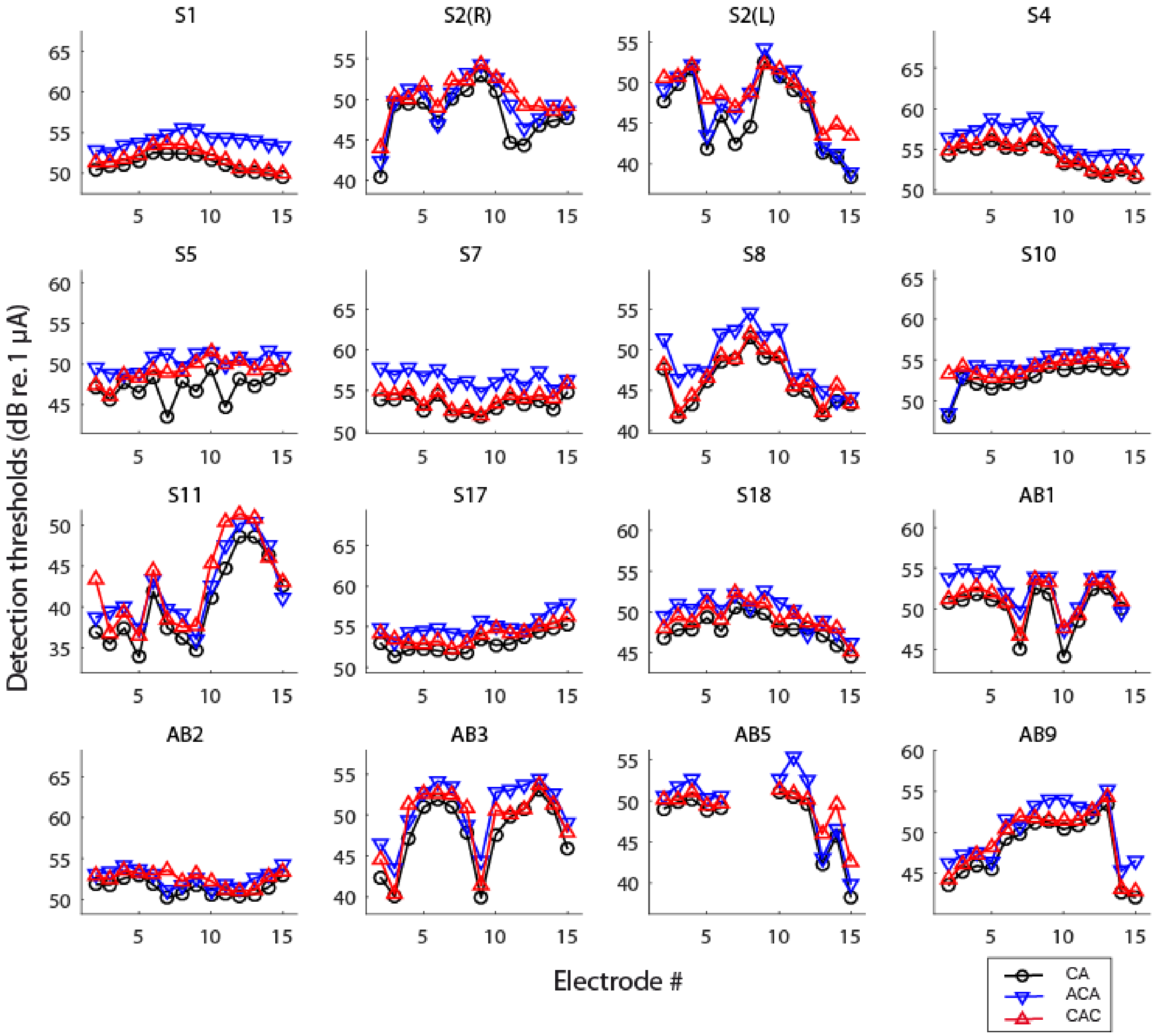

Figure 3: Detection thresholds (in decibels re. 1 μA) obtained for all pulse shapes (CA, ACA, and CAC) using pTP stimulation. Each panel is for one subject.

3.1.1 Polarity effect

CA-thresholds were always lower or equal to anodic (CAC) and cathodic (ACA) thresholds. This finding is predicted by the simple linear filter model of Carlyon et al., (2005) which accounts for the smoothing of the stimulus waveform at the level of the cell membrane. It may also relate to the fact that with CA pulses, both polarities are more likely to initiate action potentials (Coste and Pfingst, (1996); Undurraga et al., (2013)) and/or that triphasic pulses contain two phase reversals instead of one, which reduces the effect of the central phase (van Wieringen et al., (2008)). Polarity sensitivity was quantified by calculating the polarity effect, PE, defined as the difference in dB between cathodic and anodic thresholds. As a result, negative values of PE indicate that, for a given electrode, the cathodic threshold is lower than the anodic threshold. Figure 4 displays the individual across-electrode patterns of PE. Overall, out of 219 electrodes, 48 (22%) yielded negative PE (see figure 4). For each subject, we calculated the average of PE across the electrode array, referred to as $\overline{\mathrm{PE}}$ which can be considered as a global measure of polarity sensitivity. The average polarity effect ($\overline{\mathrm{PE}}$) was 0.87 dB and a sign test showed that across this group of CI users, the effect was more likely to be positive than negative (df = 15, p = 0.021). In other words, anodic thresholds were significantly more likely to be lower than cathodic thresholds for this group of CI users. Individual t-tests performed for each subject, on PE, yielded similar conclusions for ten out of sixteen ears tested. The polarity effect was not significantly different from zero for S2(L), S10, S11, AB2 and AB5. It was significantly negative for S2(R) (p=0.04).

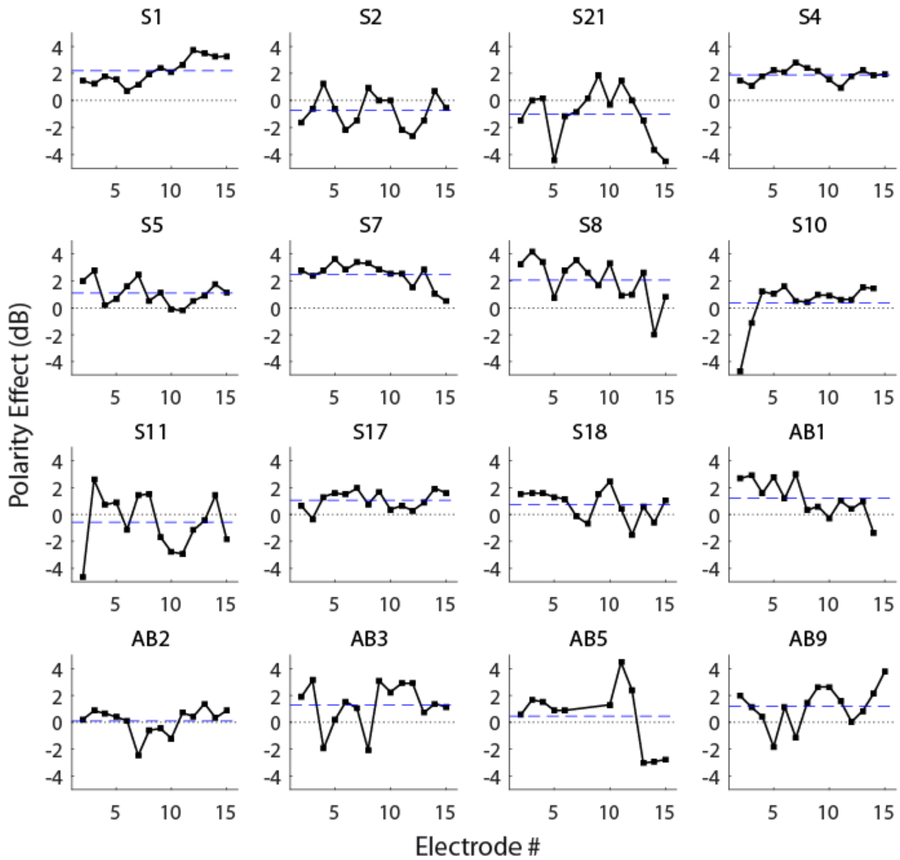

Figure 4: Across-electrode pattern of polarity effects obtained for each subject (Difference between cathodic and anodic thresholds in dB). Dotted lines indicate the 0 dB baseline. Dashed lines represent the mean PE.

If cathodic stimulation preferentially initiates action potentials at the level of the peripheral processes, the negative PE obtained for 48 of the electrodes tested may indicate that more peripheral processes are present in such cases. By extension, it may also imply that neural health ~~survival~~ is better near these electrodes.

The data were first averaged across the array for each subject. Pearson's correlations revealed a significant positive relationship between the mean thresholds with CA pulses and the mean polarity effect (r=0.50, df=14, p=0.047; Figure 5.A). However, this relationship might be partly driven by the left-most point on figure 5.A (+ symbol, corresponding to subject S11).

A weak but significant correlation was also observed at the within-subject level (ie. after removing the between-subject variance, Bland and Altman, (1995)) (r=0.19, df=201, p=0.006, Figure 5.B). These results indicate that the polarity effect might explain a small part of the between- and within-subject variance in thresholds, and are broadly consistent with the findings of Carlyon et al., (2018), and Jahn and Arenberg (2019)

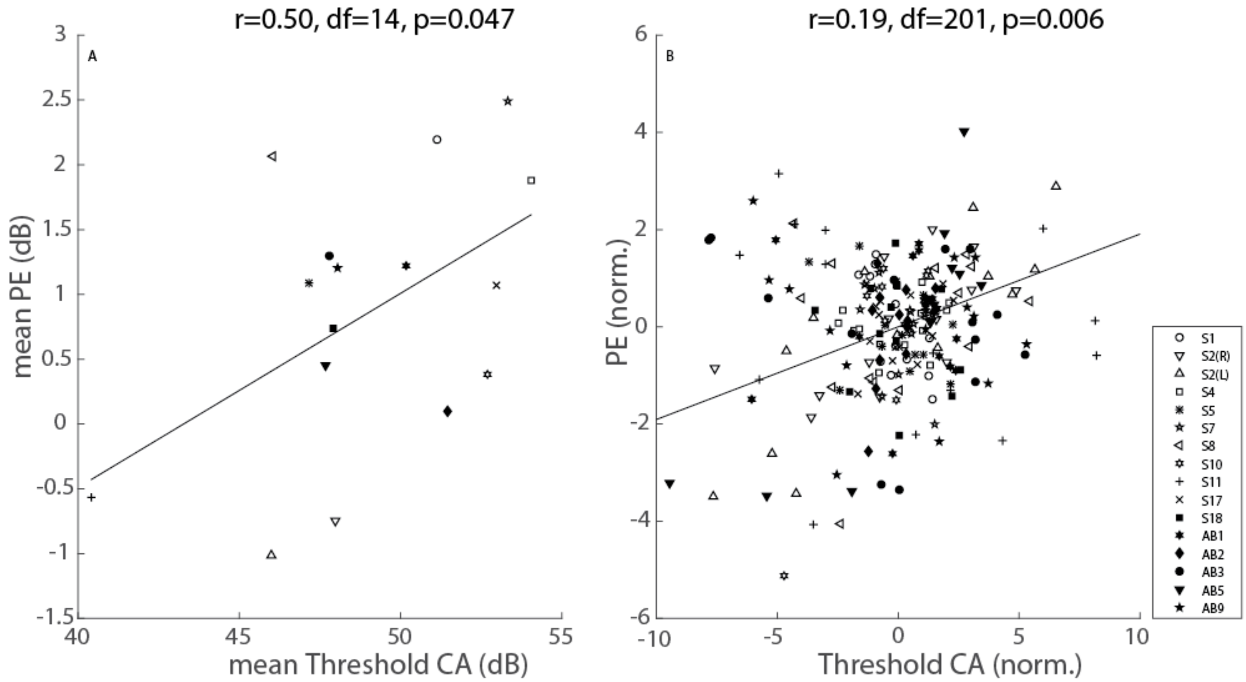

Figure 5: Panel A: Mean polarity effect (dB) as a function of the mean detection threshold (dB). Panel B: Normalized polarity effect as a function of the detection threshold (dB) measured with CA pulses, also normalized. Each symbol is for one subject

CT scans enabled the identification of irregular positions of some electrodes. S5 had his three or four most basal electrodes located inside the scala vestibuli. For S11, we spotted a tip fold-over on electrodes 1 and 2 (most apical). This subject also showed a large difference in polarity effect between electrodes 2 and 3, but it remains difficult to assess if this resulted from this abnormal positioning. As a matter of verification, the same analysis as in fig. 5 was carried out without these abnormally located electrodes. The within-subject correlation was still significant (r=0.20, df=197, p=0.005) but the between-subject correlation did not remain significant (r=0.48, df=14, p=0.052).

3.1.2 The effect of EMD

We assessed the reliability of EMD estimations using the methods described in Bland and Altman, (1999). Figure 6.A represents the EMDs reported by Observer 2 as a function of the EMDs reported by Observer 1 (r=0.83) . Figure 6.B illustrates the difference in EMDs between the two observers as a function of the average EMD from both observers, with dotted lines indicating the 95% confidence interval. Estimations within the confidence interval were averaged while the 6 electrodes falling beyond the confidence limits were not considered in the following statistical analyses.

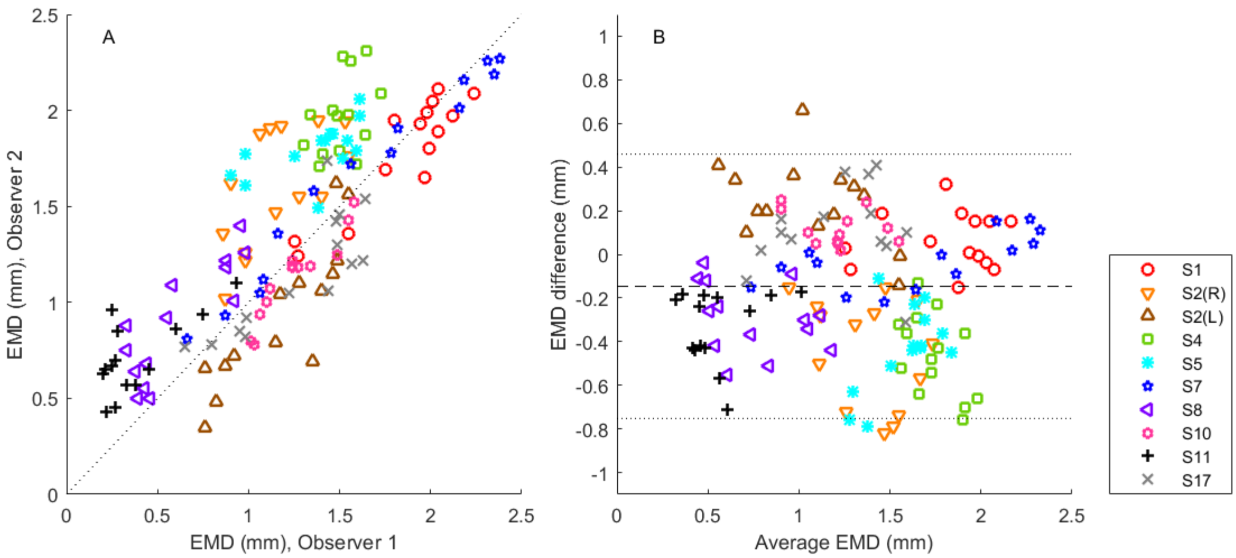

Figure 6: Panel A: EMD estimations from Observer 2 as a function of the EMD estimations from Observe 1 (mm). Dotted line represents the equality line. Panel B: EMD difference between the two observers as a function of the EMD averaged across the two observers. The dashed line represents the mean of the whole data set (-0.14 mm, the average absolute difference was 0.27 mm). The dotted lines represent the 95% confidence interval.

Figure 7 shows the individual EMD estimations as a function of the electrode number. Across the ten subjects for whom cone-beam CT scans were available, EMD estimates ranged between 0.32 and 2.33 mm, consistent with the observation of Jahn and Arenberg, (2019) for the same make of CIs.

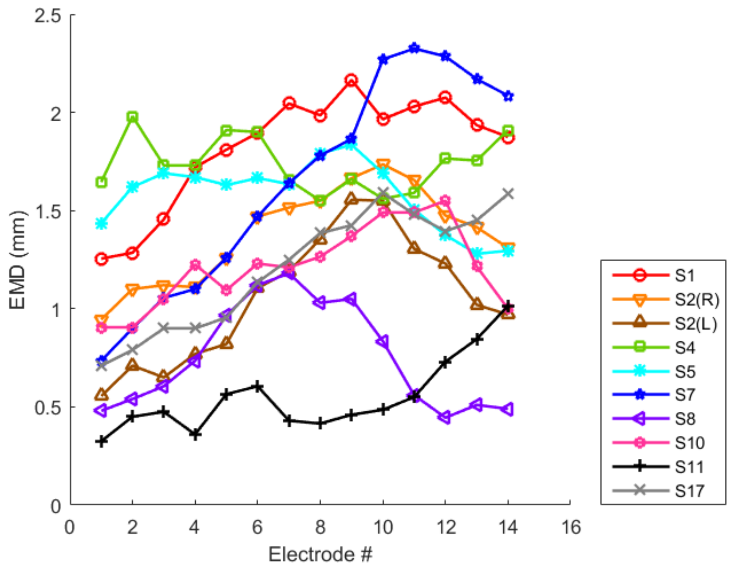

Figure 7: EMD estimations (mm) as a function of electrode number.

To analyze the between-subject variance in threshold, we calculated the mean threshold (across the array) and the mean EMD (across the array) for these 10 subjects. Figure 8 shows the variation of the mean threshold as a function of the mean EMD. Each symbol is for one subject. For all three pulse shapes, a significant positive correlation was found between EMDs and detection thresholds (df = 8, $p<0.05$; see figure 8). This model accounts for 52, 55 and 58% of the between-subject variance in thresholds for CA, ACA and CAC stimuli respectively. The EMD and the threshold patterns for each subject were then normalized by their mean value across the electrode array to pool the data from all subjects together and perform a within-subject correlation analysis. Figure 9 represents the normalized thresholds as a function of the EMD for the three pulse shapes. It shows that on average, only a small part of the within-subject variance in threshold can be explained by the EMD (average r=0.28, df =120, p<0.01). This poor relationship may be due to a small within-subject variability in EMD values. In other words, for any given subject, the EMD was relatively homogeneous across the electrode array but it could differ across

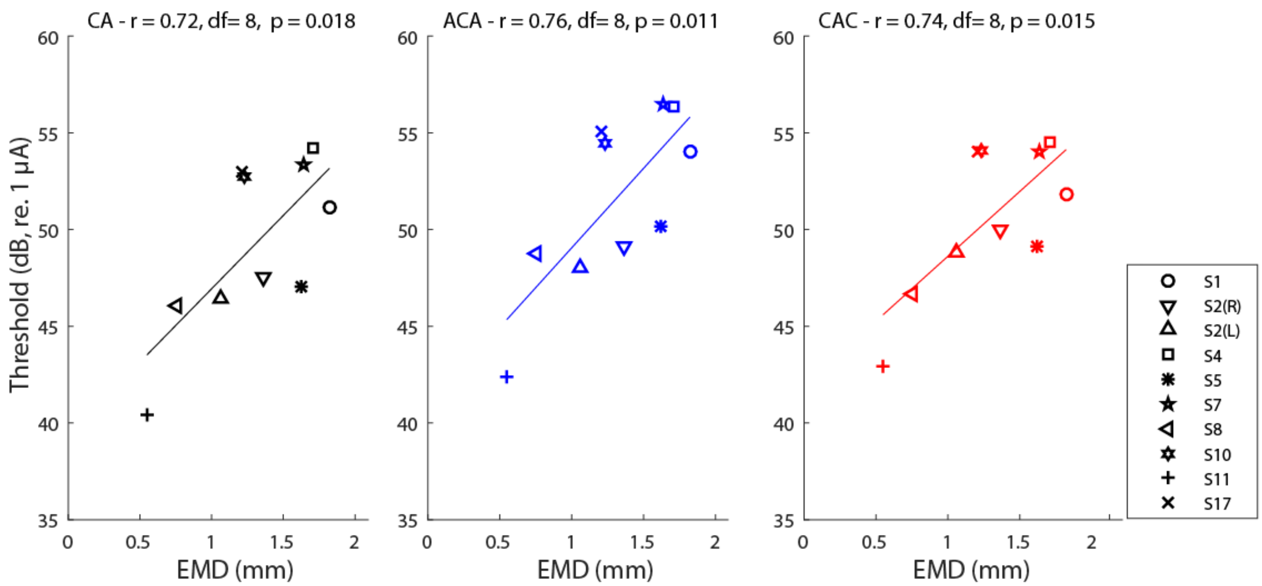

Figure 8: Mean detection threshold (dB) as a function of mean EMD (mm), averaged across the array. Each symbol is for one subject. Different panels illustrate the relationship for the three different pulse shapes CA, ACA and CAC.

subjects. For each subject, the difference in EMD between electrodes was smaller in our subject group (between 0.43 mm and 1.59 mm depending on the subject, 0.82 mm on average) than in Long et al., (2014), (0.75mm to 1.45mm, 1.20mm on average). This discrepancy will be discussed in section 4.

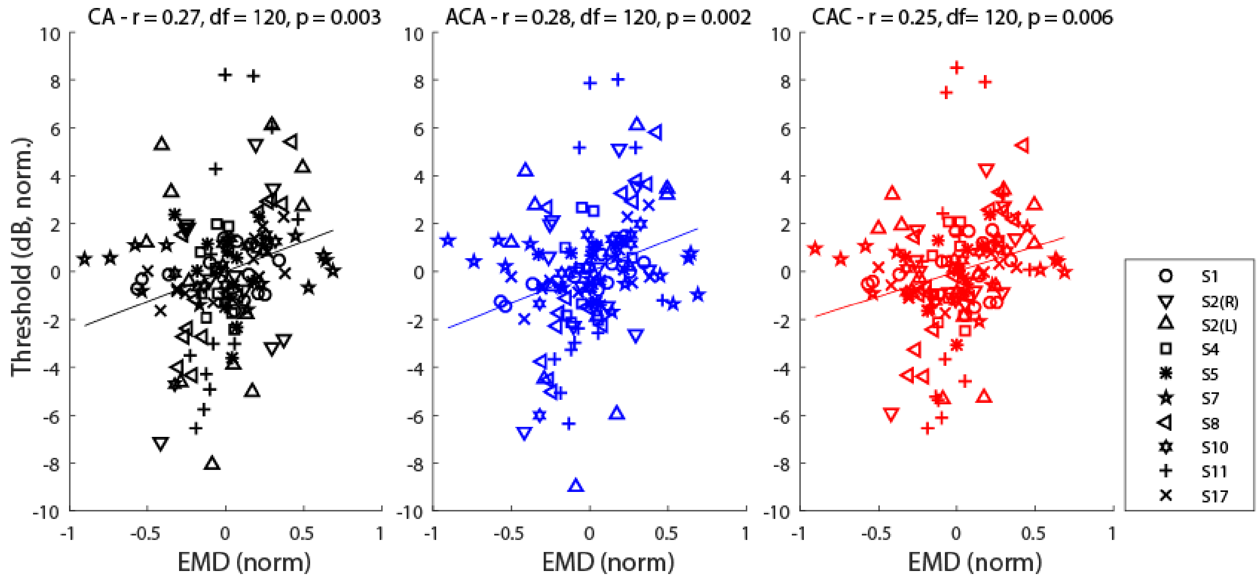

Figure 9: Normalized thresholds as a function of the normalized EMD. Each symbol is for one subject. Different panels illustrate the relationship for the three different pulse shapes CA, ACA and CAC.

3.1.3 Relationship between EMD, the polarity effect, and detection thresholds

The present findings suggest that both the EMD and PE have an influence on detection thresholds. However, the model study by Rattay, et al., (2001) suggested that polarity sensitivity may be influenced by the position of the electrode relative to the nerve fibers. It thus remains unclear whether the proportions of the threshold variance explained by these two parameters overlap. To investigate the combined contribution of EMD and PE on detection thresholds, partial correlation analyses were performed and the results are reported in Table 2. It indicates that detection thresholds correlate with both the EMDs and PEs and that each factor could only explain 6.5 and 4% of the variance respectively (when partialling out PE and the EMD, respectively).

It is also worth noting that no relationship was found between the EMDs and the PE when the detection thresholds were partialled out. We also fitted our data using a multilevel regression model which corroborated this finding (MLWin software, Rasbash et al., (2009), results not shown here). It therefore shows that both the EMD and PE contribute to explain some of the variance of the across-electrode threshold patterns.

3.2 Supra-threshold tasks

3.2.1 Speech recognition

Word recognition scores ranged from 20% to 68% with an average score of 43.2% for French speaking participants and 66.6% for English speaking participants. The test/retest reliability, expressed as the percentage of variation between the two lists, ranged between 0 and 24% (12% on average for French subjects and 7% for English subjects). Individual speech recognition scores are reported in Table 1. To be able to pool the speech recognition data from all participants, the logit of the speech scores were normalized by the mean value obtained in each group. Contrary to previous studies by Pfingst et al., (2004) and Long et al., (2014), in the present data, the within-subject variance in threshold was not correlated with the normalized logit of the speech recognition scores ($r = -0.24$, $df = 12$, $p = 0.399$).

Long et al., (2014) reported that neither mean threshold alone nor mean EMD alone predicted speech recognition scores. However, in their study, the root mean square error (RMSE) of the distance model was significantly correlated with speech intelligibility. As a result, they proposed the RMSE as a metric for the prediction of CI performance. For each of our subjects, the RMSE to the global distance model presented above was calculated. However, no such correlation was observed ($r=0.19$, $df=6$, $p=0.64$).

3.2.2 SMRT

The scores of the SMRT test carried out with all subjects ranged between 0.66 and 4.01 rpo with an average score of 1.84 rpo (see individual scores in table 1). Recently, O'Brien and Winn, (2017) reported that the transmission of spectral ripples through CI processors is subject to spectral aliasing and that additional cues may be used by the subjects to perform the task above a critical ripple density value. To circumvent this problem, the SMRT scores were winsorized with a maximum value of 2 rpo (corrected mean = 1.49 rpo).

It is worth noting that the outcomes of the speech recognition and SMRT tests were not correlated. This may relate to the inherent limitations of using this spectral ripple test with CIs as reported by O'Brien and Winn, (2017) or to the fact that speech recognition is more affected by individual factors such as experience with speech. As for speech scores, SMRT scores were not correlated to the RMSE (r=0.62, df =8, p=0.101). The within-subject variance in thresholds was not correlated to the SMRT scores (r = 0.44, df = 14, p = 0.085), however, one should mention that they were surprisingly positively correlated when considering the non-winsorized SMRT scores (r=0.62, df=14, p=0.010).

3.2.3 Comparison of polarity effect and performance on supra-threshold tasks

If, as suggested by the correlation between PE and detection threshold, PE relates to neural health ~~survival~~, we would expect better performance in SMRT and speech recognition when PE is low. To evaluate this hypothesis, we consider the mean polarity effect averaged across the electrode array as previously defined. Figure 10 displays SMRT scores in rpo (Panel A), and normalized speech logit (Panel B) as a function of $\overline{\mathrm{PE}}$. We can note that SMRT scores show a significant negative relationship with $\overline{\mathrm{PE}}$ (r=-0.56, df=14, p=0.025) which corroborates our hypothesis that polarity sensitivity relates to neural health ~~survival~~. Note that very similar correlations were obtained when using the non-winsorized SMRT scores (r=-0.55, df=14, p=0.026). In contrast, no significant relationship was observed between $\overline{\mathrm{PE}}$ and normalized speech recognition scores (r=0.42, df=12, p=0.136).

Besides, to assess the robustness of this global measure of neural health ~~survival~~, the same correlation analysis was carried out for even and odd subsets of electrodes separately, which also yielded significant correlations between SMRT scores and the polarity effect (even electrode: r=-0.57, p=0.020; Odd electrodes: r=-0.52, p=0.041).

Here again these results are consistent with the hypothesis that PE relates to some aspects of neural health ~~survival~~.

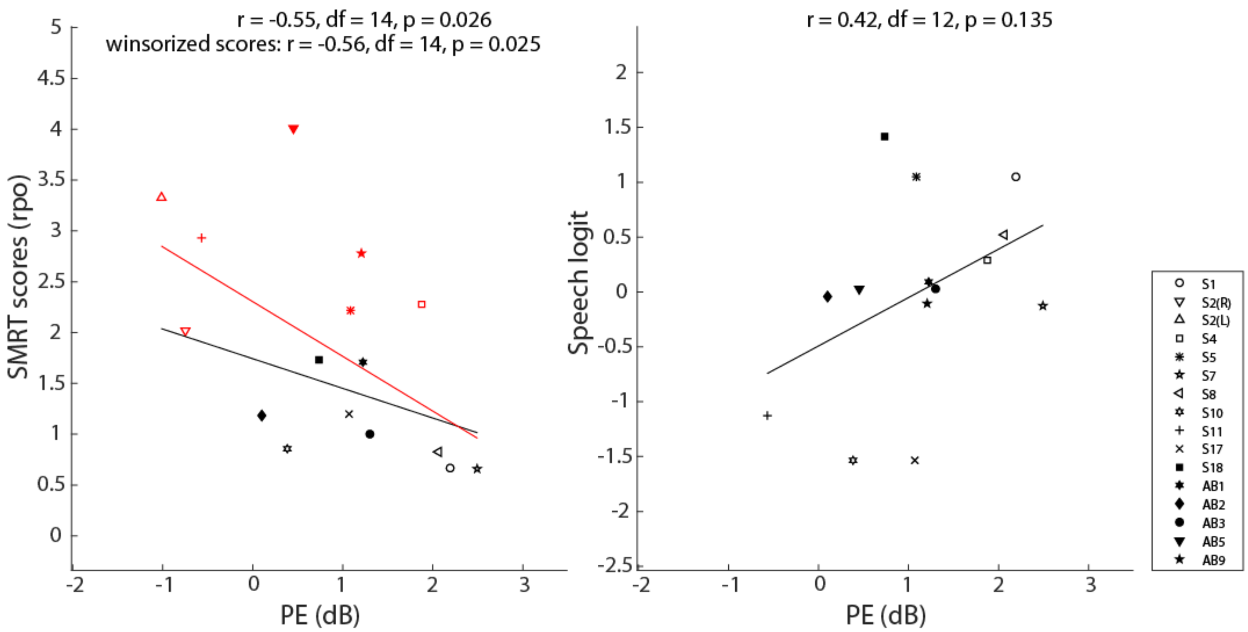

Figure 10: Panel A: SMRT scores (in ripples per octave) as a function of the difference between cathodic and anodic thresholds (in dB). Red symbols were winsorized for the correlation analysis. Panel B: Normalized logit of speech recognition scores as a function of the difference between cathodic and anodic thresholds (in dB).

4 Discussion and conclusion

We measured detection thresholds in CI users and tried to explain the across- and within-subject variability. In particular, we aimed to assess the influence of two potential factors on these detection thresholds ~~the role of two potential factors influencing the neural responsiveness~~: a measure of the distance between the electrodes and the nerve fibers, and a proposed psychophysical correlate of neural health ~~survival~~. We tried to understand to what extent these factors relate to detection thresholds.

(1) Across-site variance in thresholds

Previous studies showed that speech performance is negatively correlated with the across-site variance in thresholds (Pfingst et al., (2004); Bierer, (2007); Long et al., (2014)). This measure of variance was thus proposed as a potential correlate of neural health ~~survival~~. As in DeVries and Arenberg, (2018), speech test outcomes in the present experiment did not replicate those findings. Several factors may have influenced this lack of relationship. First, those earlier studies were conducted with a different device and different speech materials. Second, although Long et al., (2014) used a CNC word recognition test which is close to what was done in the present study, their subject group was also larger and more homogeneous than ours. In the present study, speech testing was carried out with the subjects' own processor meaning that the device settings/parameters differed across subjects. Furthermore, their experience with their device varied from 0.5 to 15 years. In contrast, in Long et al., (2014), all speech recognition tests were carried out 12 months post-activation and using the same external processor for all subjects, thereby providing the exact same stimulation strategy (Monopolar stimulation and ACE strategy). This might have reduced the number of subject-specific parameters that could influence speech recognition. Finally, the stimulation mode might play an important role since Long et al., (2014) found a significant relationship for PA and bipolar stimulation but not for tripolar and monopolar stimulation modes. In their study, monopolar stimulation yielded rather homogeneous across-electrode thresholds compared to PA (the within-subject variance in thresholds was 2.25 dB^2 on average for monopolar and 34.8 dB^2 for PA). In the present study, the average variance in thresholds using pTP stimulation was 8 dB^2. This relatively small variance might explain why it did not correlate with speech performance in the present study but did in their study with PA stimulation.

(2) Electrode-to-modiolar wall distance (EMD)

Consistent with several previous studies, we showed that the distance to the modiolar wall (i.e. near where the neurons lie) has an influence on detection threshold (Cohen et al., (2006); Long et al., (2014)). More specifically, we found that the distance model could explain 54% of the between-subject variance in thresholds but only 7% of the within-subject variance. As previously mentioned, this difference may result from the relatively small across-site variance in EMDs for our group of subjects.

Consistent with this observation, at the individual level, the so-called distance model was only significant for four of the ten subjects (S8, S10, S11 and S17). It is worth noting that in Long et al., (2014), a significant relationship was observed for seven of ten subjects with the phased-array electrode configuration (PA) and for only four of them with MP configuration. Another important factor might be that in their study all subjects were users of the Nucleus® perimodiolar electrode array while in the present study, only S2(L), S8 and S11 were implanted with an electrode array meant to be close to the modiolus (i.e. a HiFocus 1j with a positioner or a midscala electrode array).

Furthermore, we did not replicate the finding that speech scores correlate with the RMSE of the distance model.

Despite the difference in electrode configuration, one may wonder whether the acuracy of the EMD estimations might have affected the present results. Long et al., (2014) used a more advanced procedure for the estimation of the EMD. First, the resolution of our CT images was slightly poorer compared to Long et al., (2014) (125μm cubic voxels versus 100μm in their study). In particular, the localization of the modiolar wall in the apical region was sometimes difficult due to a poor contrast and the presence of artifacts. Second, Long et al., (2014) had access to either pre-operative scans that were not contaminated by electrode artifacts, or to a scalable cochlear model, which was not our case. This resulted in a relatively large variability in the EMD estimations from both observers. While it was verified that the analysis conducted with each set of estimations yielded consitent results, it may be possible that this variability reduced the significance of the EMD as an explanatory factor for the variance in detection thresholds.

(3) Polarity sensitivity

Macherey et al., (2008) originally reported that human CI users consistently show a higher sensitivity to anodic stimulation at MCL. Other recent studies (Macherey et al., (2017); Carlyon et al., (2018); Goehring et al., (2019); Jahn and Arenberg, (2019)) reported that some subjects and/or electrodes may also exhibit a polarity sensitivity at threshold, which is reliable but can be in either direction. In the present study we analyzed a relatively large number of measurements which revealed a higher sensitivity to anodic stimulation for 78% of the tested electrodes at threshold.

Similar to the results of Jahn and Arenberg, (2019), who used the same methods for threshold measurements but using monopolar stimulation, no relationship was found between EMDs and the polarity effect. The partial correlations analysis suggests that both the EMD and PE contribute to the variance in thresholds. ~~play a role in the neural responsiveness~~.

From previous modeling studies (Rattay, et al., (2001); Resnick et al., (2018)), the difference between cathodic and anodic thresholds, PE is assumed to reflect the degree of degeneration or demyelination of the peripheral processes. In particular, high values of PE may relate to a place where peripheral processes cannot be stimulated or are degenerated. Interestingly, SMRT scores and $\overline{\mathrm{PE}}$ were negatively correlated. Even though the part of the variance in SMRT explained by $\overline{\mathrm{PE}}$ was small (31%), this result is consistent with this hypothesis.

(4) Perspectives

Even though we found that both the EMD and the polarity effect might contribute to explain this variance in threshold at both the between- and within-subject levels, the correlations were weak. This means that there may be other more central factors that are important and/or that polarity sensitivity only represents one aspect of neural health ~~survival~~ (e.g. survival of peripheral processes but not overall health ~~survival~~).

Another limitation of the present result is that our analysis of the relationship between the performance on suprathreshold tasks and the polarity sensitivity only considered $\overline{\mathrm{PE}}$ which is averaged across the entire array and thus removes the information of the across-electrode differences in PE. It might thus be interesting to replicate this experiment with subsets of electrodes which exhibit little variation in PE to investigate the effect of polarity on performance in a within-subject analysis. Additional factors still need to be identified to better explain those results, these might for instance include the amount of fibrosis and/or ossification.

CT-scan analysis only enabled an estimation of the distance between the electrodes and the modiolar wall. A higher resolution might have enabled measurement not only of the EMD but also of the distance to the osseous spiral lamina (OSL). This distance may better represent the potential excitation site on the peripheral processes and also better relate to polarity sensitivity, as reported by Rattay, et al., (2001). In this case it would have been interesting to test the distance model on the one hand, between the EMD and anodic thresholds and, on the other hand, between the distance to the OSL and cathodic thresholds.

Although further investigation is required to strengthen the observation made in the present study, our results add some evidence that polarity sensitivity reflects some aspects of the electrode-neuron interface that have functional/perceptual implications (Carlyon et al., (2018); Hughes et al., (2018); Goehring et al, 2019). Being able to picture the places where healthy neurons lie may be beneficial for the optimization of stimulation strategies. In particular, current focusing and current steering techniques using multipolar strategies have been investigated in the past to create spatially selective virtual channels and thus improve spectral resolution (Berenstein et al., (2008); Bonham and Litvak, (2008)). While it was demonstrated that the locus of excitation might be slightly shifted by manipulating the amplitude of different electrodes, the benefits in terms of speech recognition were small or inconsistent across studies and/or subjects. The polarity effect might provide relevant information to further improve such strategies. It might also be used to select specific electrodes in order to target regions of the cochlea where the neural population is expected to be healthy.

Acknowledgments

We sincerely thank Alan Archer-Boyd, John Deeks, Debbie Vickers, Jean-Pierre Piron, Marielle Sicard, for their help with the data collection in Cambridge and in France and the CI participants for their work. This study was partly funded by Advanced Bionics.

Subjects	Duration of deafness prior to CI (years)	Etiology	CI use (years)	Age (years)	Deactivated electrodes	Speech scores (%)	SMRT scores (rpo)
S1	20	Unknown progressive	12	38	None	60	0.67
S2(R)	7	Unknown progressive	7	62	None	n/a	2.02
S2(L)	1	Unknown progressive	1	62	None	n/a	3.33
S4	10	Unknown progressive	13	52	None	47	2.28
S5	6	Usher syndrome	13	20	None	60	2.22
S7	24	Pendred syndrome	12	39	None	40	0.66
S8	2	Unknown progressive	15	87	None	51	0.83
S10	47	Ototoxicity following meningitis	12	61	E16	20	0.86
S11	34	Congenital	0.5	42	None	25	2.93
S17	10	Viral	11	63	None	20	1.20
S18	20	Possible ototoxicity	1.5	35	None	66	1.93
AB5	18	Otosclerosis	6	73	E8	67	4.01
AB1	n/a	n/a	7	71	E15	68	1.71
AB9	n/a	n/a	2	71	None	65	2.78
AB2	16	Acquired, possible	8	57	None	66	1.18

		ototoxicity					
AB3	33	Otosclerosis	8	70	None	67	1.00

Table 1: Subjects details. Subjects labelled with S- were tested in France, and those labelled with AB- were tested in the United Kingdom.

Variables	Control	r	df	p
Threshold, EMD	**PE**	0.25	117	0.006*
Threshold, PE	**EMD**	0.20	117	0.029*
EMD, PE	**Threshold**	0.06	117	0.516

Table 2: Partial correlations statistics.

Bibliography

Aronoff, and Landsberger. (2013). The development of a modified spectral ripple test. *The Journal of the Acoustical Society of America*, *134*(2), EL217-22. http://doi.org/10.1121/1.4813802

Berenstein, Mens, Mulder, and Vanpoucke. (2008). Current Steering and Current Focusing in Cochlear Implants : Comparison of Monopolar , Tripolar , and Virtual Channel Electrode Configurations. *Ear and Hearing*, *29*(2), 250–260.

Bierer. (2007). Threshold and channel interaction in cochlear implant users: evaluation of the tripolar electrode configuration. *The Journal of the Acoustical Society of America*, *121*(3), 1642–53. http://doi.org/10.1121/1.2436712

Bierer, Bierer, and Middlebrooks. (2011). Partial tripolar cochlear implant stimulation: Spread of excitation and forward masking in the inferior colliculus. *Hearing Research*, *4*(164), 134–142. http://doi.org/10.1126/scisignal.2001449.Engineering

Bierer, and Faulkner. (2010). Identifying cochlear implant channels with poor electrode-neuron interface: partial tripolar, single-channel thresholds and psychophysical tuning curves. *Ear and Hearing*, *4*(164), 247–258. http://doi.org/10.1126/scisignal.2001449.Engineering

Blamey, Artieres, Başkent, Bergeron, Beynon, Burke, … Lazard. (2013). Factors affecting auditory performance of postlinguistically deaf adults using cochlear implants: An update with 2251 patients. *Audiology and Neurotology*, *18*(1), 36–47. http://doi.org/10.1159/000343189

Bland, and Altman. (1995). Calculating correlation coefficients with repeated observations: Part 1 - correlation within subjects. *BMJ*, *310*, 446.

Bland, and Altman. (1999). Measuring agreement in method comparison studies with heteroscedastic measurements. *Statistical Methods in Medical Research*, *8*, 135–160. http://doi.org/10.1002/sim.5955

Bonham, and Litvak. (2008). Current Focusing and Steering. *Hearing Research*, *242*((1-2)), 141–153. http://doi.org/10.1016/j.heares.2008.03.006.

Bonnet, Frijns, Peeters, and Briaire. (2004). Speech recognition with a cochlear implant using triphasic charge-balanced pulses. *Acta Oto-Laryngologica*, *124*(4), 371–375. http://doi.org/10.1080/00016480410031084

Carlyon, Cosentino, Deeks, Parkinson, and Arenberg. (2018). Effect of Stimulus Polarity on Detection Thresholds in Cochlear Implant Users: Relationships with Average Threshold, Gap Detection, and Rate Discrimination. *JARO - Journal of the Association for Research in Otolaryngology*, *19*(5), 559–567. http://doi.org/10.1007/s10162-018-0677-5

Carlyon, Deeks, and Macherey. (2013). Polarity effects on place pitch and loudness for three cochlear-implant designs and at different cochlear sites. *The Journal of the Acoustical Society of America*, *134*(1), 503–509. http://doi.org/10.1121/1.4807900

Carlyon, van Wieringen, Deeks, Long, Lyzenga, and Wouters. (2005). Effect of inter-phase gap on the sensitivity of cochlear implant users to electrical stimulation. *Hearing Research*, *205*(1–2), 210–224. http://doi.org/10.1016/j.heares.2005.03.021

Cohen, Saunders, Knight, and Cowan. (2006). Psychophysical measures in patients fitted with Contour and straight Nucleus electrode arrays. *Hearing Research*, *212*(1–2), 160–75. http://doi.org/10.1016/j.heares.2005.11.005

Cosentino, Gaudrain, Deeks, and Carlyon. (2016). Multistage nonlinear optimization to recover neural activation patterns from evoked compound action potentials of cochlear implant users. *IEEE Transactions on Biomedical Engineering*, *63*(4), 833–840.

http://doi.org/10.1109/TBME.2015.2476373

Coste, and Pfingst. (1996). Stimulus features affecting psychophysical detection thresholds for electrical stimulation of the cochlea. III. Pulse polarity. *The Journal of the Acoustical Society of America*, *99*(5), 3099–3108. http://doi.org/10.1121/1.414796

DeVries, and Arenberg. (2018). Current Focusing to Reduce Channel Interaction for Distant Electrodes in Cochlear Implant Programs. *Trends in Hearing*, *22*, 1–18. http://doi.org/10.1177/2331216518813811

Eddington, Tierney, Noel, Hermann, Whearty, and Finley. (2004). *Speech processors for auditory prostheses. Ninth quarterly progress report, NIH contract N01-DC-2-1001,Neural Prosthesis Program, National Institutes of Health, Bethesda, MD*.

Escudé, James, Deguine, Cochard, Eter, and Fraysse. (2006). The size of the cochlea and predictions of insertion depth angles for cochlear implant electrodes. *Audiology and Neurotology*, *11*(SUPPL. 1), 27–33. http://doi.org/10.1159/000095611

Fayad, and Linthicum. (2006). Multichannel cochlear implants: Relation of histopathology to performance. *Laryngoscope*, *116*(8), 1310–1320. http://doi.org/10.1097/01.mlg.0000227176.09500.28

Garadat, Litovsky, Yu, and Zeng. (2010). Effects of simulated spectral holes on speech intelligibility and spatial release from masking under binaural and monaural listening. *The Journal of the Acoustical Society of America*, *127*(2), 977–989. http://doi.org/10.1121/1.3273897

Glueckert, Pfaller, Kinnefors, Rask-Andersen, and Schrott-Fischer. (2005). The human spiral ganglion: New insights into ultrastructure, survival rate and implications for cochlear implants. *Audiology and Neurotology*, *10*(5), 258–273. http://doi.org/10.1159/000086000

Goehring, Archer-Boyd, Deeks, Arenberg, and Carlyon. (2019). A Site-Selection Strategy Based on Polarity Sensitivity for Cochlear Implants: Effects on Spectro-Temporal Resolution and Speech Perception. *JARO - Journal of the Association for Research in Otolaryngology*, *20*(4), 431–448. http://doi.org/10.1007/s10162-019-00724-4

Hughes, Choi, and Glickman. (2018). What can stimulus polarity and interphase gap tell us about auditory nerve function in cochlear-implant recipients? *Hearing Research*, *359*, 50–63.

http://doi.org/10.1016/j.heares.2017.12.015

Jahn, and Arenberg. (2019). Evaluating Psychophysical Polarity Sensitivity as an Indirect Estimate of Neural Status in Cochlear Implant Listeners. *JARO - Journal of the Association for Research in Otolaryngology*. http://doi.org/10.1007/s10162-019-00718-2

Jolly, Spelman, and Clopton. (1996). Quadrupolar Stimulation for Cochlear Prostheses : Modeling and Experimental Data. *IEEE Transactions on Biomedical Engineering*, *43*(8), 857–865.

Kamakura, and Nadol. (2016). Correlation between word recognition score and intracochlear new bone and fibrous tissue after cochlear implantation in the human. *Hearing Research*. http://doi.org/10.1016/j.heares.2016.06.015

Khan, Handzel, Burgess, Damian, Eddington, and Nadol. (2005). Is Word Recognition Correlated With the Number of Surviving Spiral Ganglion Cells and Electrode Insertion Depth in Human Subjects With Cochlear Implants? *Laryngoscope*, *115*(April), 672–677.

Landsberger, Padilla, and Srinivasan. (2012). Reducing Current Spread using Current Focusing in Cochlear Implant Users. *Hearing Research*, *284*, 16–24. http://doi.org/10.1016/j.heares.2011.12.009.Reducing

Lawler, Yu, and Aronoff. (2017). HHS Public Access. *Ear and Hearing*, *38*(6), 760–766. http://doi.org/10.1097/AUD.0000000000000496

Linthicum, and Anderson. (1991). Cochlear Implantation of Totally Deaf Ears : Histologic Evaluation of Candidacy Cochlear Implantation of Totally Deaf Ears. *Acta Oto-Laryngologica*, *111*(2), 327–331. http://doi.org/10.3109/00016489109137395

Litvak. (2003). *BEDCS Bionic Ear Data Collection System. Version 1.16, user manual*.

Litvak, Spahr, and Emadi. (2007). Loudness growth observed under partially tripolar stimulation: model and data from cochlear implant listeners. *The Journal of the Acoustical Society of America*, *122*(2), 967–81. http://doi.org/10.1121/1.2749414

Long, Holden, McClelland, Parkinson, Shelton, Kelsall, and Smith. (2014). Examining the electro-neural interface of cochlear implant users using psychophysics, CT scans, and speech understanding. *Journal of the Association for Research in Otolaryngology*, *15*(2), 293–304. http://doi.org/10.1007/s10162-013-0437-5

Macherey, Carlyon, Chatron, and Roman. (2017). Effect of Pulse Polarity on Thresholds and on Non-monotonic Loudness Growth in Cochlear Implant Users. *JARO - Journal of the Association for Research in Otolaryngology*, *18*(3), 513–527. http://doi.org/10.1007/s10162-016-0614-4

Macherey, Carlyon, van Wieringen, Deeks, and Wouters. (2008). Higher sensitivity of human auditory nerve fibers to positive electrical currents. *Journal of the Association for Research in Otolaryngology : JARO*, *9*(2), 241–51. http://doi.org/10.1007/s10162-008-0112-4

Macherey, and Cazals. (2016). Effects of Pulse Shape and Polarity on Sensitivity to Cochlear Implant Stimulation : A Chronic Study in Guinea Pigs. *Advances in Expe*. http://doi.org/10.1007/978-3-319-25474-6

Macherey, van Wieringen, Carlyon, Deeks, and Wouters. (2006). Asymmetric pulses in cochlear implants: effects of pulse shape, polarity, and rate. *Journal of the Association for Research in Otolaryngology : JARO*, *7*(3), 253–66. http://doi.org/10.1007/s10162-006-0040-0

Mesnildrey, Macherey, Herzog, and Venail. (2019). Impedance measures for a better understanding of the electrical stimulation of the inner ear. *Journal of Neural Engineering*, *16*(1). http://doi.org/10.1088/1741-2552/aaecff

Micco, and Richter. (2006). Electrical resistivity measurements in the mammalian cochlea after neural degeneration. *The Laryngoscope*, *116*(8), 1334–1341. http://doi.org/10.1097/01.mlg.0000231828.37699.ab

Nadol, and Eddington. (2006). Histopathology of the Inner Ear Relevant to Cochlear Implantation. *Adv Otorhinolaryngol*, *64*, 31–39.

Nadol, Young, and Glynn. (1989). Survival of Spiral ganglion cells in profound Sensorineural hearing Loss : Implications for Cochlear Implantation. *Annals of Otology, Rhinology and Laryngology*, *98*, 411–416.

O'Brien, and Winn. (2017). Aliasing of spectral ripples through Speech, CI processors: A challenge to the interpretation of correlation with recognition scores. *Conference on Implantable Auditory Prostheses.*, *014309*(2007), 14309.

Pelliccia, Venail, Bonafé, Makeieff, Iannetti, Bartolomeo, and Mondain. (2014). Cochlea size variability and implications in clinical practice. *Acta Otorhinolaryngologica Italica : Organo*

727 *Ufficiale Della Società Italiana Di Otorinolaringologia e Chirurgia Cervico-Facciale*, *34*, 42–9.
728 Retrieved from
729 http://www.pubmedcentral.nih.gov/articlerender.fcgi?artid=3970226&tool=pmcentrez&re
730 ndertype=abstract
731 Pfingst, Colesa, Hembrador, Kang, Middlebrooks, Raphael, and Su. (2011). Detection of pulse
732 trains in the electrically stimulated cochlea : Effects of cochlear health a). *Journal of the*
733 *Acoustical Society of America*, *130*(December), 3954–3968.
734 http://doi.org/10.1121/1.3651820
735 Pfingst, Xu, and Thompson. (2004). Across-Site Threshold Variation in Cochlear Implants:
736 Relation to Speech Recognition. *Audiology and Neurotology*, *9*(6), 341–352.
737 Prado-Guitierrez, Fewster, Heasman, McKay, and Shepherd. (2007). Effect of interphase gap and
738 pulse duration on electrically evoked potentials is correlated with auditory nerve survival.
739 *Hearing Research*, *215*, 47–55.
740 Ramekers, Versnel, Strahl, Smeets, Klis, and Grolman. (2014). Auditory-nerve responses to
741 varied inter-phase gap and phase duration of the electric pulse stimulus as predictors for
742 neuronal degeneration. *JARO - Journal of the Association for Research in Otolaryngology*,
743 *15*(2), 187–202. http://doi.org/10.1007/s10162-013-0440-x
744 Rasbash, Charlton, Browne, Healy, and Cameron. (2009). MLwiN Version 2.1. Centre for
745 Multilevel Modelling, University of Bristol.
746 Rattay. (1999). The basic mechanism for the electrical stimulation of the nervous system.
747 *Neuroscience*, *89*(2), 335–346.
748 Rattay, Leao, and Felix. (2001). A model of the electrically excited human cochlear neuron. II.
749 Influence of the three-dimensional cochlear structure on neural excitability. *Hearing*
750 *Research*, *153*(1–2), 64–79.
751 Rattay, Lutter, and Felix. (2001). A model of the electrically excited human cochlear neuronI.
752 Contribution of neural substructures to the generation and propagation of spikes. *Hearing*
753 *Research*, *153*(1–2), 43–63.
754 Resnick, O'Brien, and Rubinstein. (2018). Simulated auditory nerve axon demyelination alters
755 sensitivity and response timing to extracellular stimulation. *Hearing Research*, *361*, 121–

137. http://doi.org/10.1016/j.heares.2018.01.014

Saunders, Cohen, Aschendorff, Shapiro, Knight, Stecker, … Cowan. (2002). Threshold, comfortable level and impedance changes as a function of electrode-modiolar distance. *Ear and Hearing*, *23*, 28S-40S. http://doi.org/10.1097/00003446-200202001-00004

Spelman, Clopton, and Pfingst. (1982). Tissue Impedance and Current Flow in the Implanted Ear Implications for the Cochlear Prosthesis. *Annals of Otology, Rhinology and Laryngology*, *suppl*(98), 3–8. Retrieved from http://www.ncbi.nlm.nih.gov/pubmed/?term=Tissue+Impedance+and+Current+Flow+in+the+Implanted+Ear+Implications+for+the+Cochlear+Prosthesis

Spoendlin. (1975). Retrograde degeneration of the cochlear nerve. *Acta Oto-Laryngologica*, *79*(3–6), 266–275. http://doi.org/10.3109/00016487509124683

Undurraga, Carlyon, Wouters, and van Wieringen. (2013). The Polarity Sensitivity of the Electrically Stimulated Human Auditory Nerve Measured at the Level of the Brainstem. *JARO - Journal of the Association for Research in Otolaryngology*, *14*, 359–377. http://doi.org/10.1007/s10162-013-0377-0

van der Marel, Briaire, Verbist, Muurling, and Frijns. (2015). The Influence of Cochlear Implant Electrode Position on Performance. *Audiology and Neurotology*, *20*(3), 202–211. http://doi.org/10.1159/000377616

van Wieringen, Macherey, Carlyon, Deeks, and Wouters. (2008). Alternative pulse shapes in electrical hearing. *Hearing Research*, *242*(1–2), 154–163. http://doi.org/10.1016/j.heares.2008.03.005

Vanpoucke, Zarowski, and Peeters. (2004). Identification of the impedance model of an implanted cochlear prosthesis from intracochlear potential measurements. *IEEE Transactions on Bio-Medical Engineering*, *51*(12), 2174–83. http://doi.org/10.1109/TBME.2004.836518

Venail, Mathiolon, Menjot de Champfleur, Piron, Sicard, Villemus, … Uziel. (2015). Effects of Electrode Array Length on Frequency-Place Mismatch and Speech Perception with Cochlear Implants. *Audiology and Neurotology*, 102–111. http://doi.org/10.1159/000369333

Won, Drennan, and Rubinstein. (2007). Spectral-Ripple Resolution Correlates with Speech

Reception in Noise in Cochlear Implant Users. *JARO - Journal of the Association for Research in Otolaryngology*, *8*, 384–392. http://doi.org/10.1007/s10162-007-0085-8

Zhou, and Pfingst. (2014). Relationship between multipulse integration and speech recognition with cochlear implants. *Journal of the Acoustical Society of America*, *136*(September), 1257–1268. http://doi.org/10.1121/1.4890640

fig1

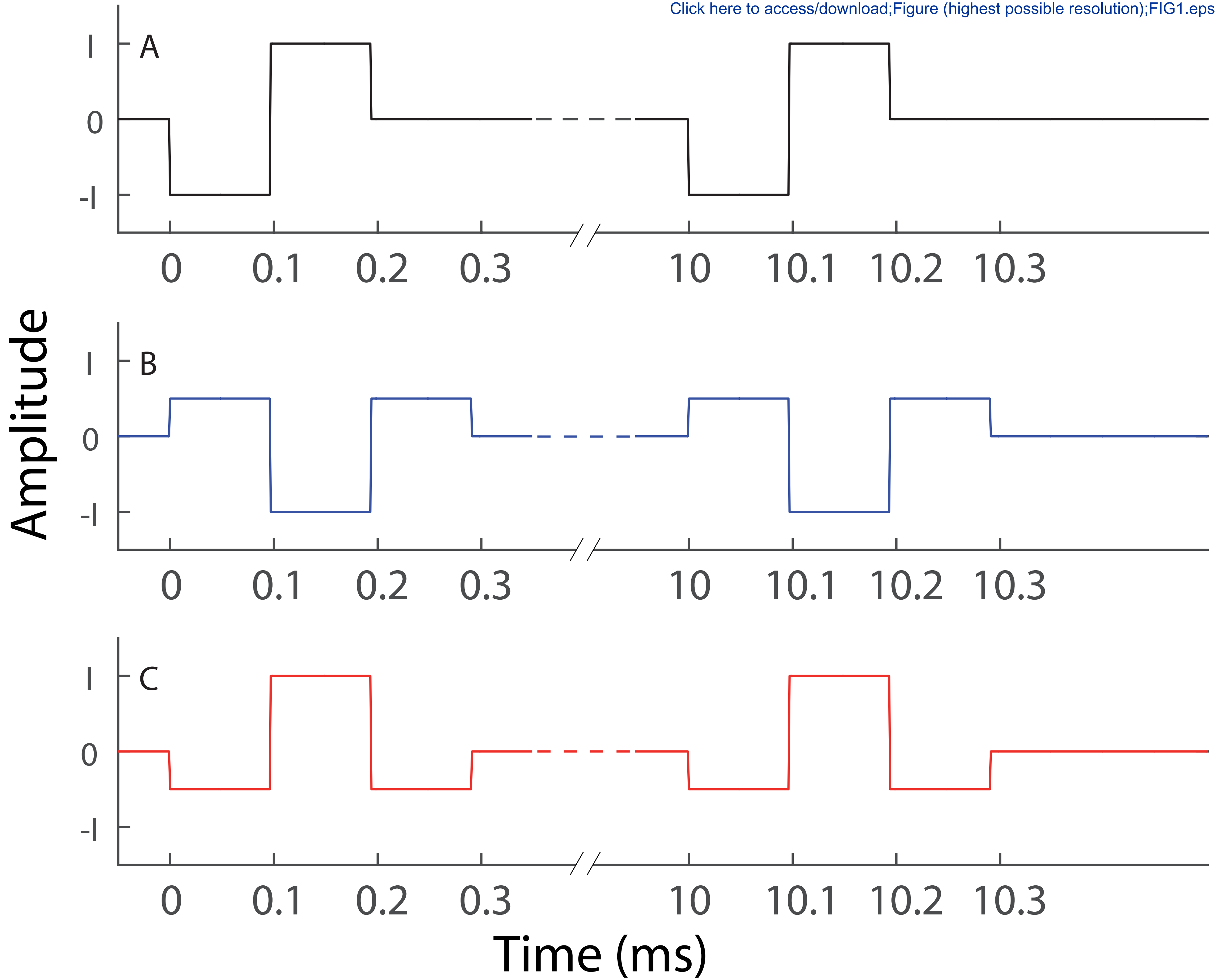

fig2 Click here to access/download;Figure (highest possible resolution);FIG2.eps

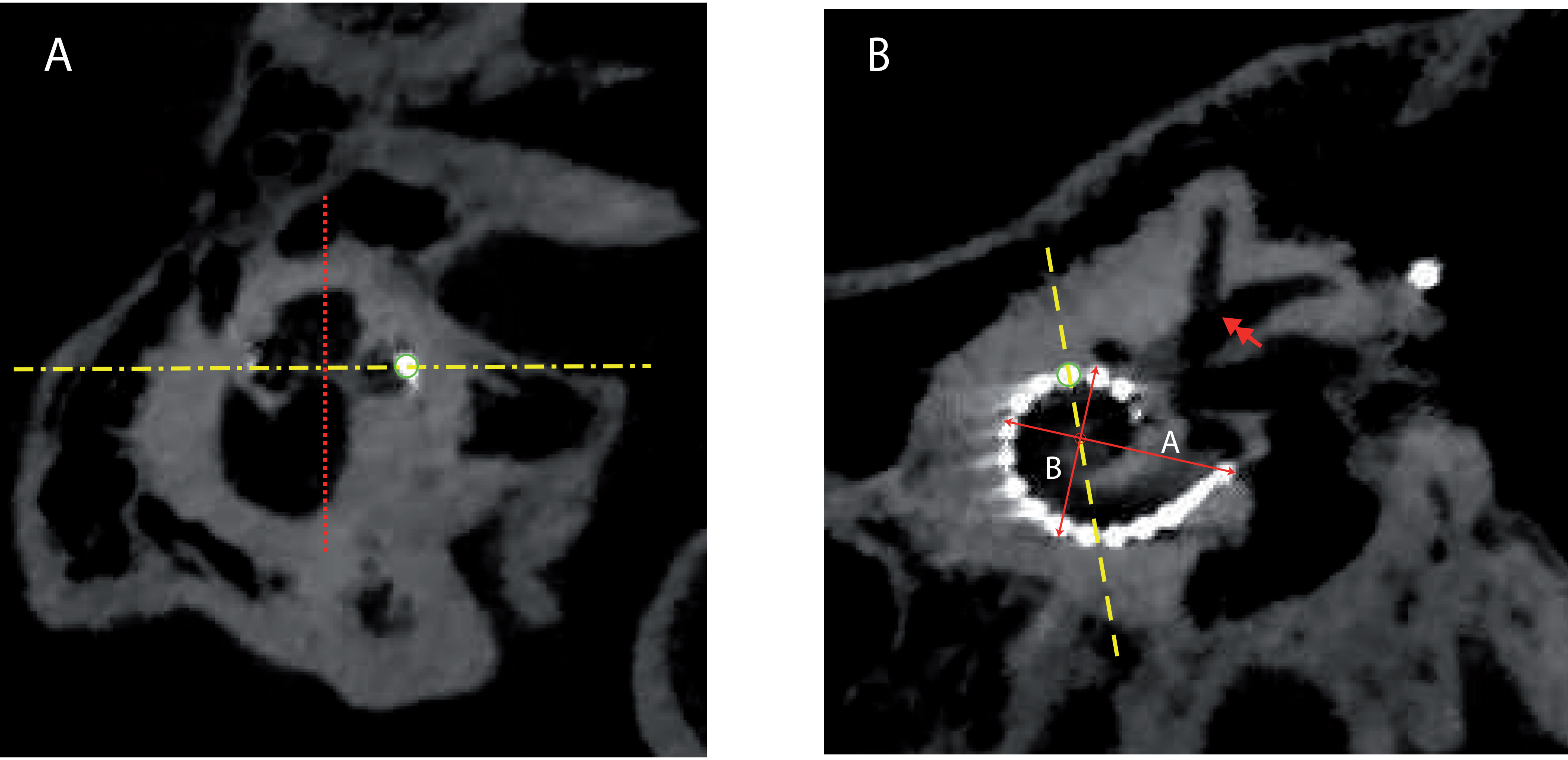

fig3

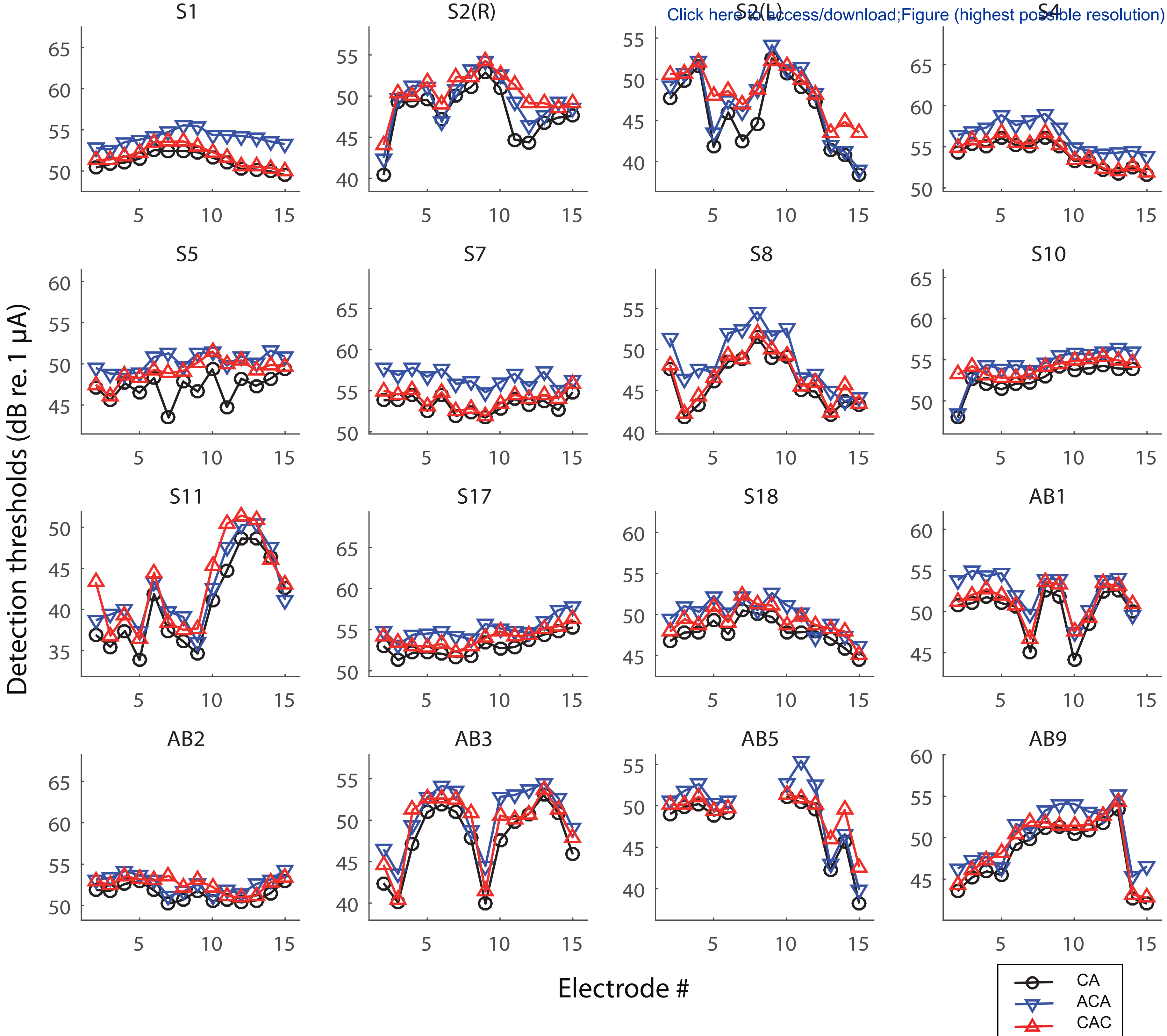
S1
S2(R)
S2(L)
S4
S5
S7
S8
S10
S11
S17
S18
AB1
AB2
AB3
AB5
AB9
Detection thresholds (dB re. 1 μA)
Electrode #
CA
ACA
CAC

fig4 Click here to access/download;Figure (highest possible resolution);FIG4.eps

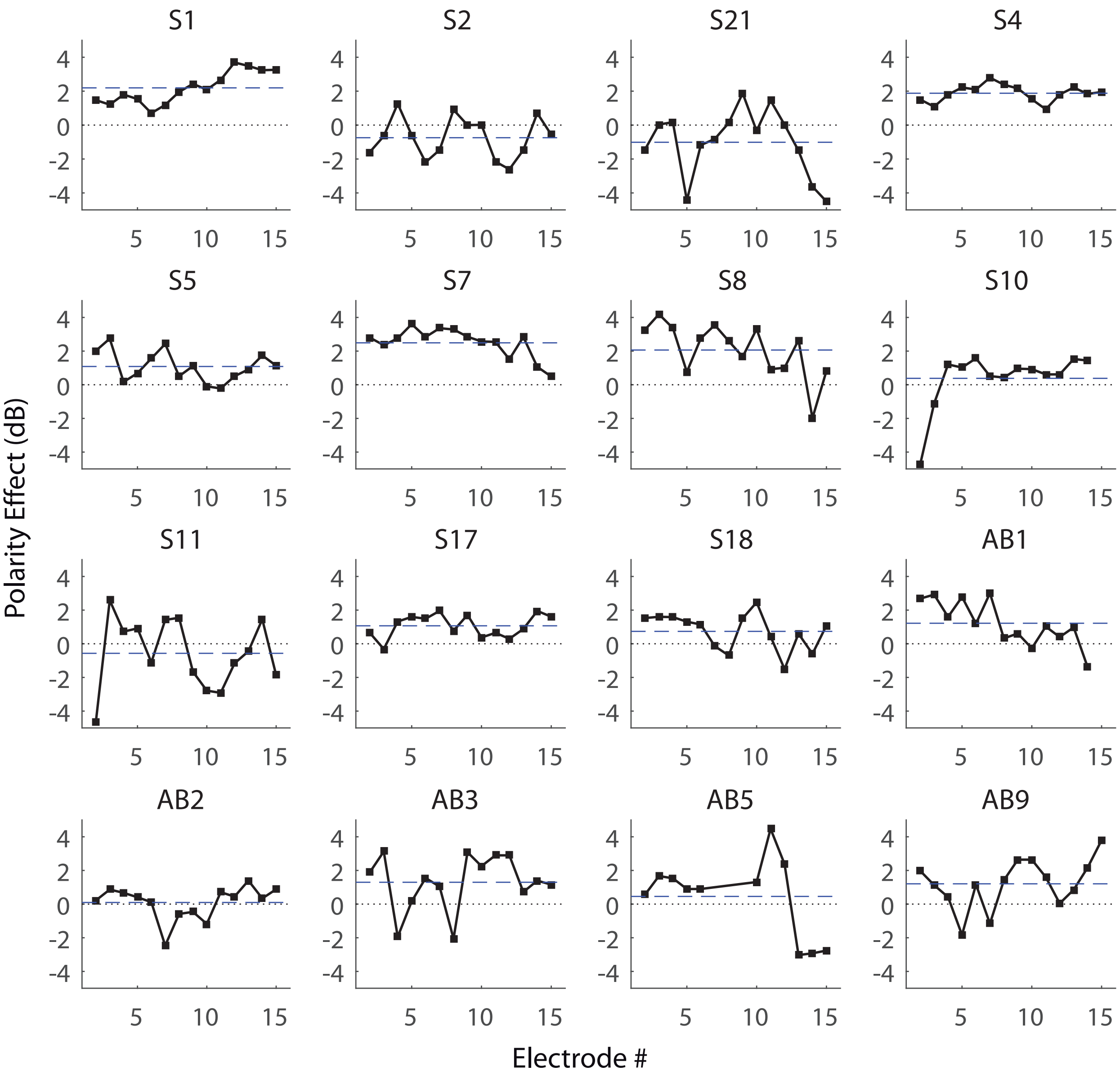

fig5

Click here to access/download;Figure (highest possible resolution);FIG5.eps

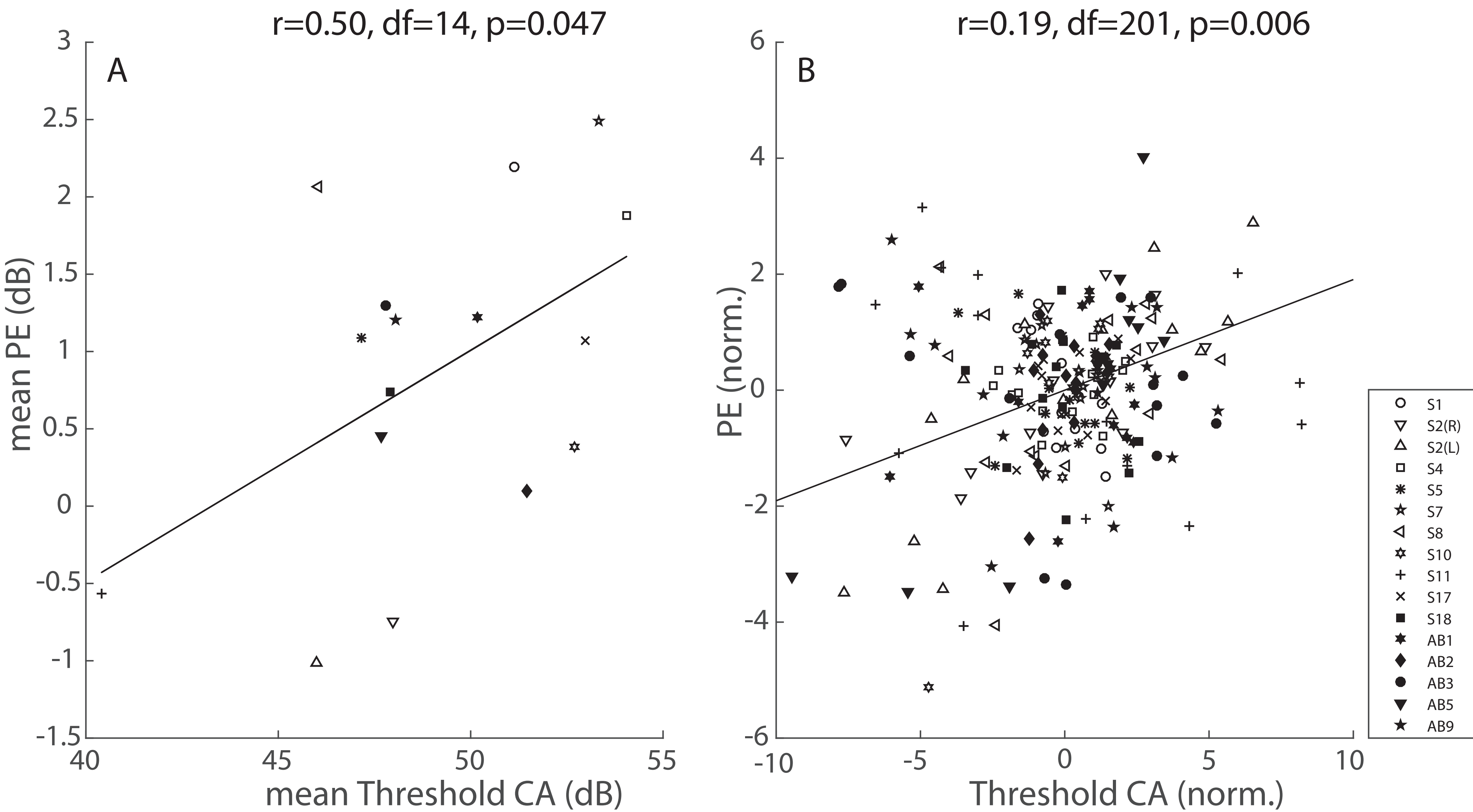

fig6

Click here to access/download;Figure (highest possible resolution);FIG6.eps

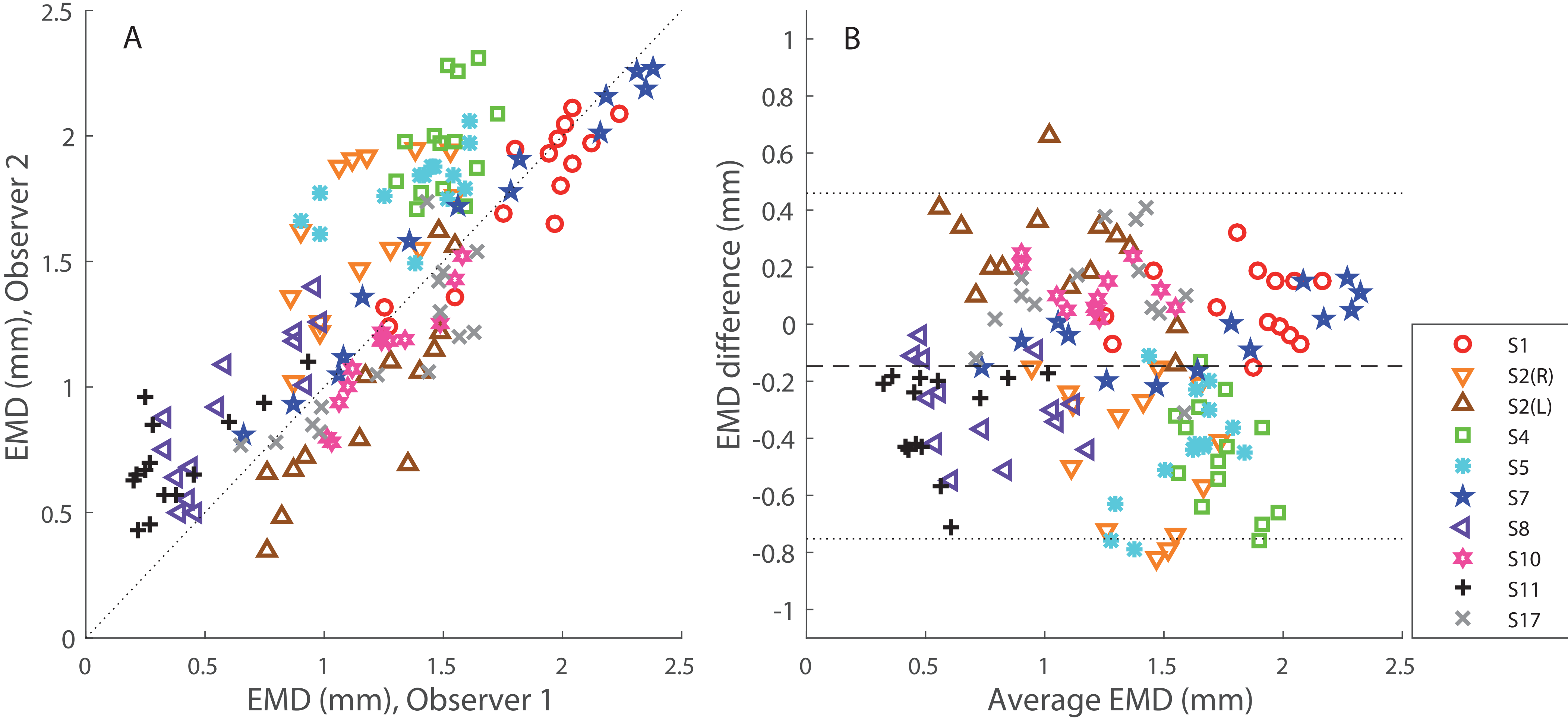

fig7

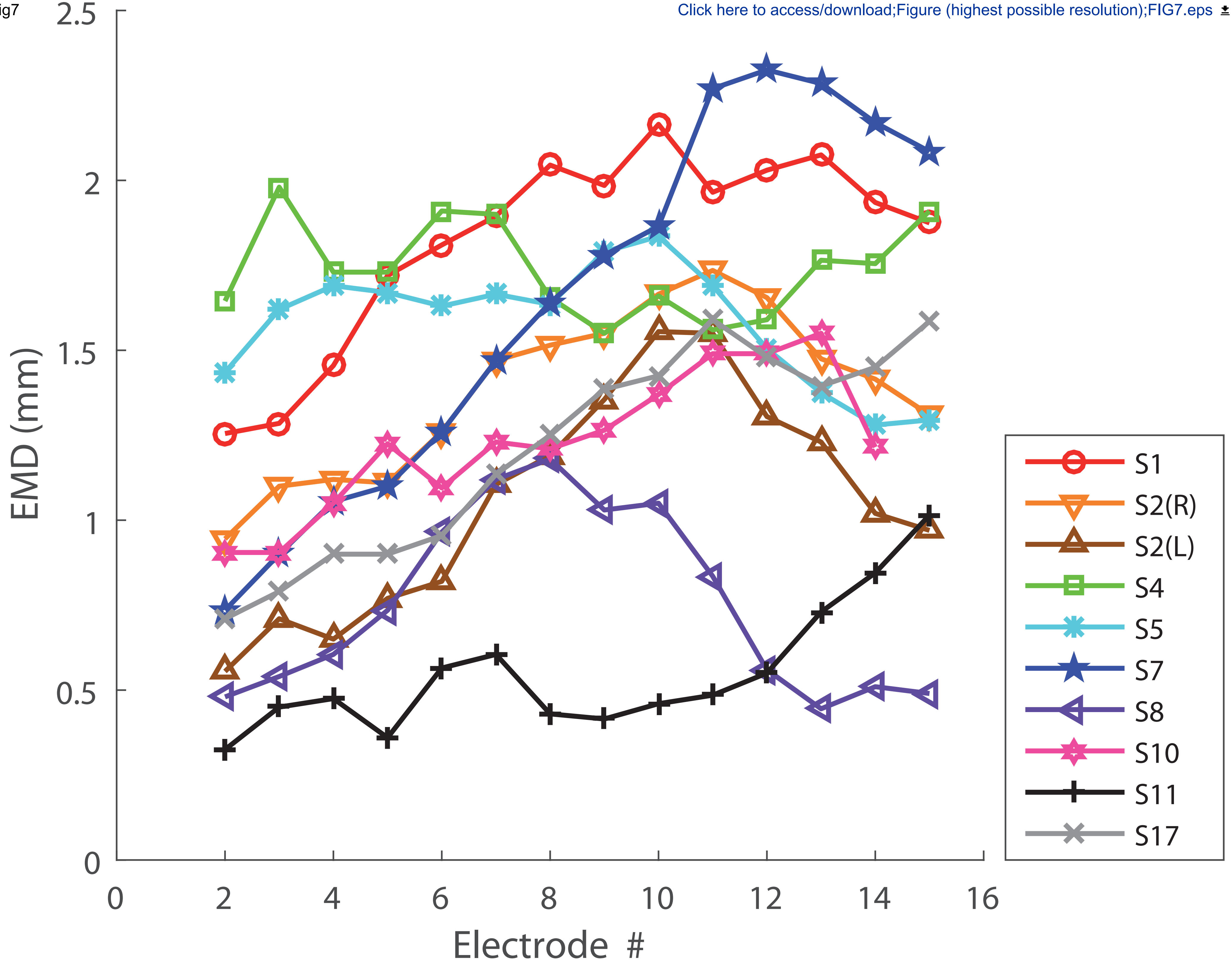
2.5
2
1.5
1
0.5
0
EMD (mm)
0
2
4
6
8
10
12
14
16
Electrode #
S1
S2(R)
S2(L)
S4
S5
S7
S8
S10
S11
S17

fig8

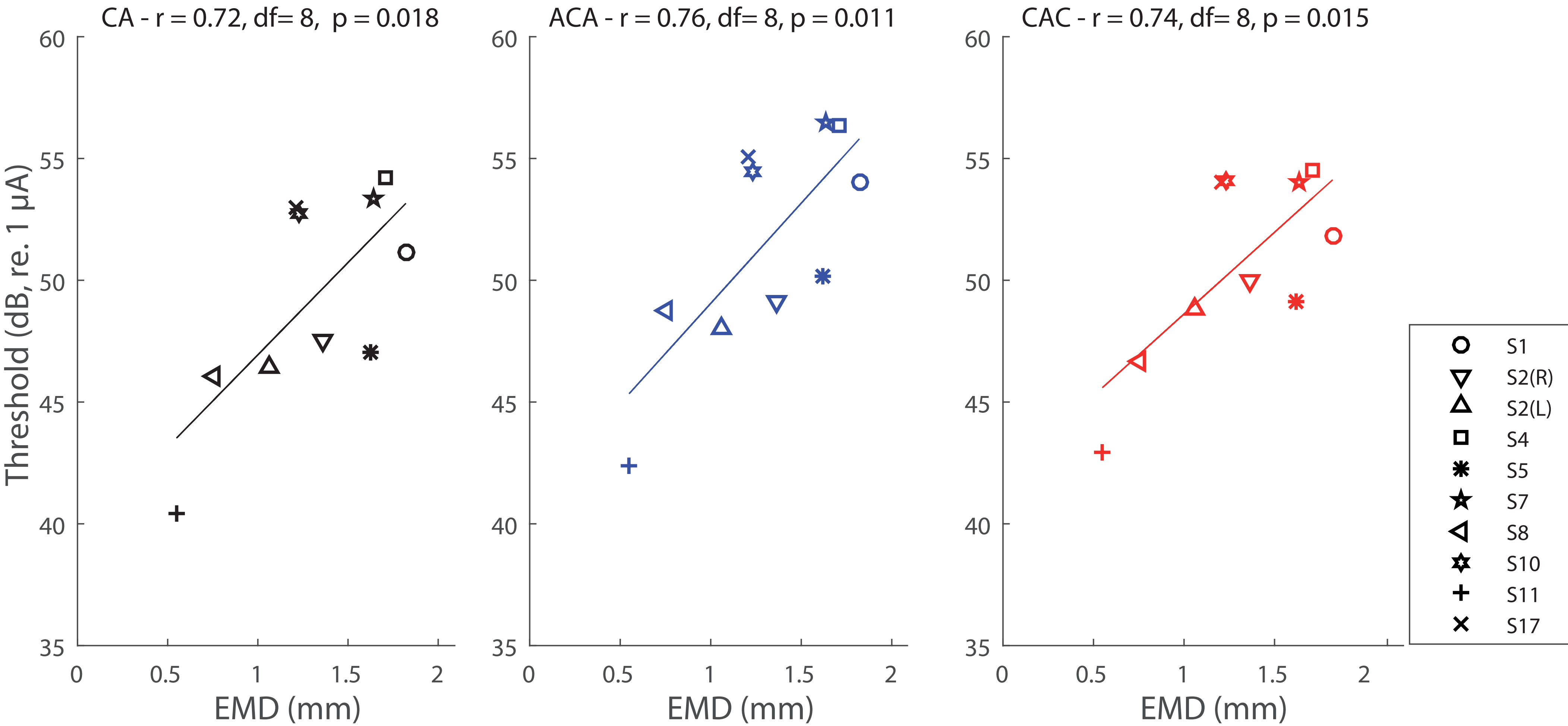

CA - r = 0.72, df= 8, p = 0.018
ACA - r = 0.76, df= 8, p = 0.011
CAC - r = 0.74, df= 8, p = 0.015
Threshold (dB, re. 1 μA)
EMD (mm)
60
55
50
45
40
35
0
0.5
1
1.5
2
S1
S2(R)
S2(L)
S4
S5
S7
S8
S10
S11
S17

fig9

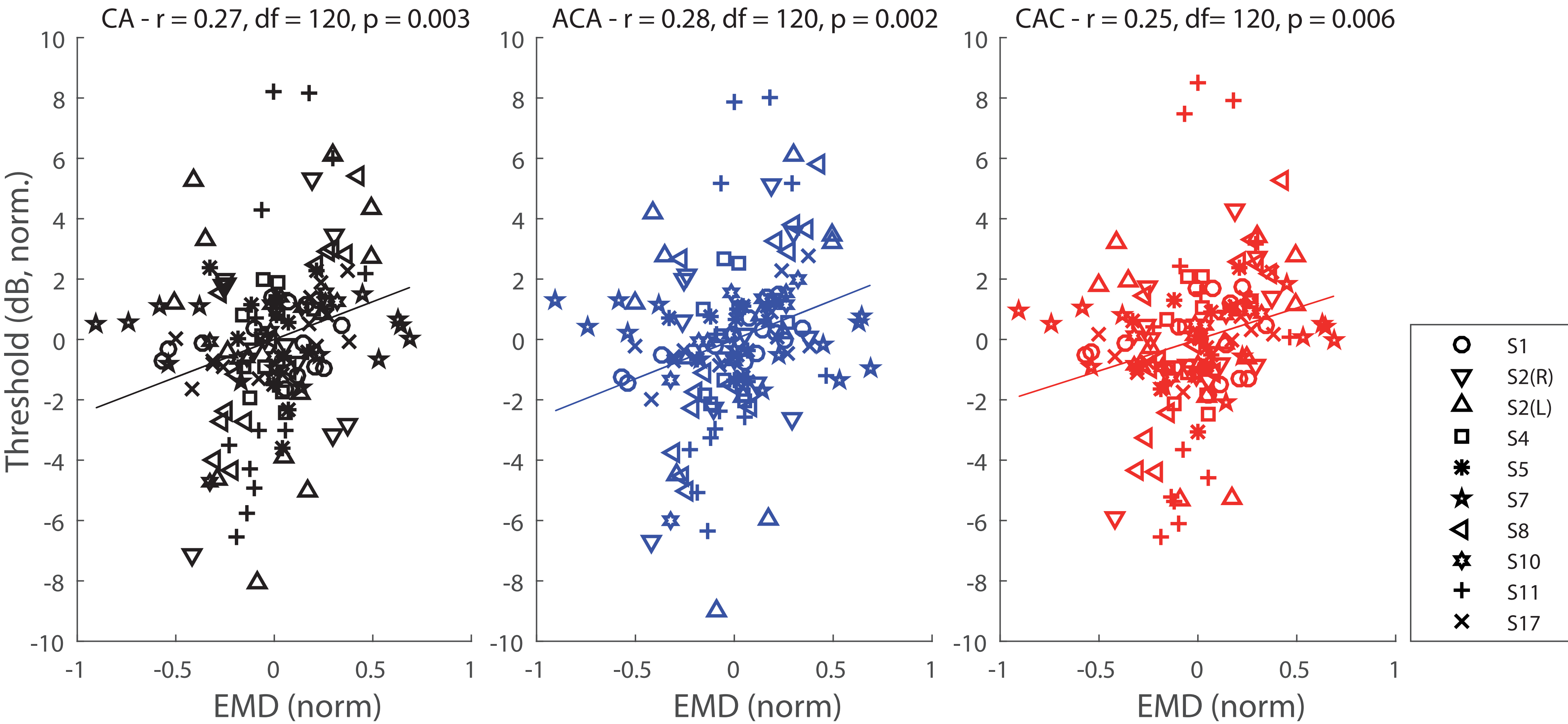
CA - r = 0.27, df = 120, p = 0.003
ACA - r = 0.28, df = 120, p = 0.002
CAC - r = 0.25, df= 120, p = 0.006
Threshold (dB, norm.)
EMD (norm)
EMD (norm)
EMD (norm)
S1
S2(R)
S2(L)
S4
S5
S7
S8
S10
S11
S17

fig10 Click here to access/download;Figure (highest possible resolution);FIG10.eps

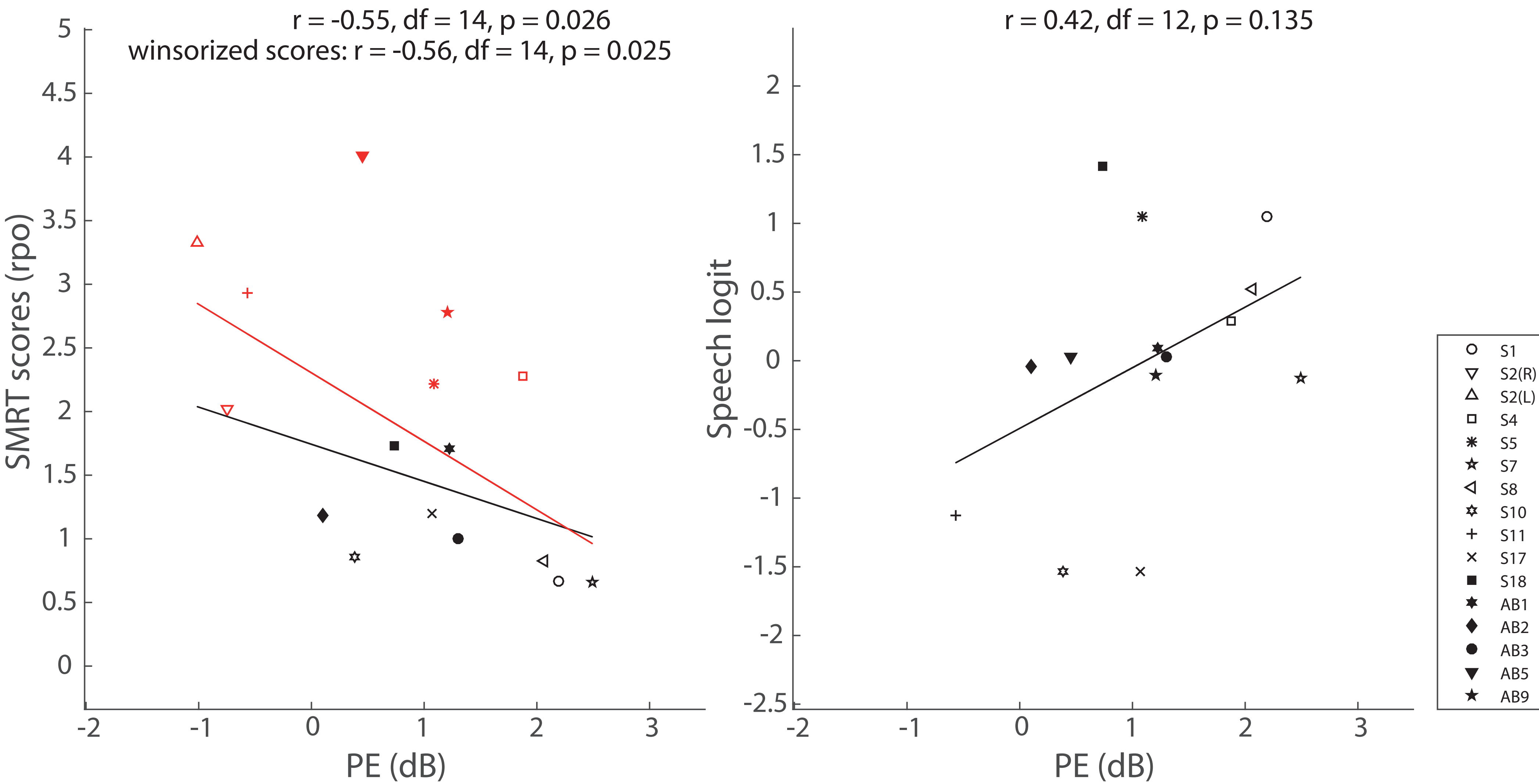

Conflict of interest statement:

The authors are fully aware of the conflict of interest policy of the journal.

We therefore declare that this work and the publication of the results is not subject to any kind of conflict of interest or copyright issues.

Sincerely yours,

Quentin Mesnildrey